Electronic Research Archive

https://www.aimspress.com/journal/era

ERA, 34(3): 1857–1884.
DOI: 10.3934/era.2026083
Received: 16 December 2025
Revised: 31 January 2026
Accepted: 10 February 2026
Published: 02 March 2026

Research article

Adaptive tracking control for multi-agent systems with deception attacks and DoS attacks

Wan Yu[1,2] **and Hui Yu**[1,2,*]

[1] Three Gorges Mathematical Research Center, China Three Gorges University, Yichang 443002, China

[2] College of Mathematics and Physics, China Three Gorges University, Yichang 443002, China

* **Correspondence:** Email: yuhui@ctgu.edu.cn.

Abstract: This paper investigates the adaptive tracking control problem for a class of strict-feedback uncertain nonlinear multi-agent systems (MASs) with input dead zones under the simultaneous presence of deception attacks and denial-of-service (DoS) attacks. A distributed leader-state estimator based on sampled data with time delays is proposed to estimate the leader's state under DoS attacks. To overcome the nonexistence of higher-order derivatives of the leader's estimated state, a filter is proposed and implemented. Based on the attacked output signals, a fuzzy state observer is constructed to reconstruct the unmeasurable states of the system. A fuzzy adaptive dead-zone control scheme is designed based on the backstepping method to mitigate the adverse effects of DoS attacks, deception attacks, dead zones, and uncertain nonlinear dynamics, while enabling the system to achieve the tracking control objective. Through Lyapunov stability analysis, the proposed control scheme is proven to guarantee that all signals in the closed-loop system are bounded and the tracking error converges to a neighborhood around the origin. Finally, simulations are conducted to verify the effectiveness of the theoretical results.

Keywords: deception attack; DoS attack; multi-agent system; adaptive tracking control; dead zone

1. Introduction

With the rapid advancement of cyber-physical system technologies, multi-agent systems (MASs) have garnered extensive attention from both academic and industrial communities [1–3], owing to their inherent advantages such as distributed collaboration, high operational efficiency, and strong adaptability. The distributed nature of MASs enables coordinated behaviors among multiple agents through local information exchange, making them particularly suitable for a variety of practical applications, including multi-unmanned aerial vehicle (UAV) formation control, autonomous robot

swarm coordination, and distributed satellite attitude synchronization [4]. Among the core challenges in MAS control, tracking control stands out as especially critical, as it requires all follower agents to converge to the trajectory generated by a leader agent while ensuring the stability and boundedness of the overall closed-loop system [5]. However, in real-world implementations, MASs often operate in complex network environments, where various uncertainties and adversarial factors pose severe threats to control reliability.

One of the major threats in such environments comes from network attacks, among which two typical types are especially prominent: deception attacks and denial-of-service (DoS) attacks [6, 7]. Deception attacks involve tampering with sensor measurements or control commands, leading to distorted state feedback and degraded control accuracy [8]. In contrast, DoS attacks disrupt communication channels by consuming limited bandwidth or blocking data transmission, causing temporary or persistent loss of leader information and inter-agent interaction signals [9, 10]. Although several studies have investigated fault-tolerant control for MASs under a single type of attack, few have addressed the combined impact of both deception and DoS attacks [11]. This represents a critical gap, since real-world cyber environments are often subject to mixed adversarial threats that simultaneously exploit multiple system vulnerabilities.

In addition to external attacks, input nonlinearities further complicate the controller design. A common issue arises from physical actuators in MASs exhibiting dead-zone nonlinearity—an inherent phenomenon where the actuator output remains zero when the input lies within a specific range [11,12]. Unlike input saturation, which has been studied in prior works, a dead zone introduces asymmetric input–output relationships and disturbance-like terms, which can easily induce oscillations or even destabilize the system if not adequately compensated [13, 14]. Although adaptive control schemes have been proposed to handle dead zones in single-agent nonlinear systems [15, 16], extending these methods to MASs under network attacks remains largely underexplored, especially given the complex coupling between attack-induced state distortion and actuator nonlinearity [17, 18].

The coexistence of deception attacks, DoS attacks, and input dead zones gives rise to a coupled challenge that drastically elevates the complexity of controller design. Deception attacks falsify measurement outputs, which not only degrades the accuracy of state observation but also impairs the effect of adaptive compensation for the nonlinear characteristics of dead zones. DoS attacks intermittently disrupt the communication topology, preventing follower agents from acquiring the state information of neighboring agents and thus necessitating the design of a resilient distributed estimator for the leader's state. When the aforementioned factors coexist, the controller is required to achieve favorable tracking control performance under the conditions of falsified measurement information, intermittent communication interruptions, and unknown input nonlinearities—a problem that has not been fully addressed in existing research.

Further challenges are posed by system uncertainties and unmeasurable states. Practical MASs often exhibit unknown nonlinear dynamics and external disturbances [19, 20], which are difficult to capture using traditional linear control approaches. To approximate such uncertainties, techniques such as fuzzy logic systems (FLSs) and neural networks are commonly employed [21]. However, integrating these tools with attack-resilient control is not straightforward. Moreover, in many real applications, only system outputs are measurable, necessitating the design of state observers to reconstruct the full state vector [22, 23]. Unfortunately, most existing observers do not adequately account for the impact of deception attacks on measurement data.

Another key bottleneck lies in distributed information acquisition under DoS attacks. When a DoS attack occurs, the communication topology of the MAS changes dynamically, and the leader's trajectory information may become unavailable to many followers [24, 25]. Conventional consensus protocols, which rely on continuous information exchange, become ineffective under intermittent communication interruptions [26]. Although distributed estimators have been proposed in the literature [25, 27], it remains challenging to ensure exponential stability of the estimation error while also addressing attack-induced time delays, such as an artificial delay [28, 29].

To address the challenges outlined above, this paper proposes an integrated adaptive tracking control scheme for nonlinear MASs subject to deception attacks, DoS attacks, and input dead zones. The main contributions of this work are summarized as follows:

1) This study investigates the tracking control problem for MASs with DoS attacks, deception attacks, uncertain nonlinear dynamics, and dead zones. A novel observer-based adaptive fuzzy tracking control scheme is proposed to enable follower agents to track a high-order leader. Unlike existing studies that only consider a single type of attack [25, 27], this paper investigates MASs subject to both DoS attacks and deception attacks. Furthermore, a more general high-order leader model is adopted herein, which is more suitable for practical application requirements compared with existing works [24, 30].

2) Based on sampled data with time delays, a distributed state estimator is proposed to estimate the leader's state. By introducing an artificial delay, the estimator ensures that the estimation error converges to zero exponentially even in the presence of DoS attacks. To address the problem that the high-order derivatives of the leader's estimated state do not exist due to DoS attacks, a filter similar to [24] is proposed herein to resolve the computational challenge of these high-order derivatives.

3) Based on the backstepping design method, the dead-zone input is well designed via a fuzzy adaptive method, and no dead-zone parameters need to be known. Unlike some existing studies [13, 14], the proposed approach does not require prior knowledge of the exact minimum of the dead-zone boundary parameters. By stability analysis, the proposed control scheme guarantees that all closed-loop system signals are bounded, and the tracking errors converge to a neighborhood around the origin.

The remainder of this paper is organized as follows: Section 2 presents preliminary knowledge, encompassing graph theory fundamentals and necessary lemmas; Section 3 formulates the problem, providing the system model to be studied and essential assumptions; Section 4 designs the leader state estimator and the filter; Section 5 constructs the observer; Section 6 develops the adaptive controller using the backstepping method; Section 7 presents the main results of this paper along with stability analysis; Section 8 validates the effectiveness of the proposed scheme through numerical simulations; finally, conclusions are drawn for the entire paper.

2. Preliminaries

Notations: $\mathbb{R}, \mathbb{R}^+, \mathbb{R}^n, \mathbb{R}^{n\times m}$, and $\mathbb{N}$ denote the sets of real numbers, non-negative real numbers, n-dimensional real vectors, $n \times m$ real matrices, and positive integer numbers, respectively. $\|\cdot\|$ denotes the 2-norm of a matrix or vector. Matrix $Q > 0$ means that Q is positive definite. $\lambda_{\min}(\cdot)$ and $\lambda_{\max}(\cdot)$ represent the minimum and maximum eigenvalues, respectively. $f^{(i)}(x)$ represents the ith derivative of

function $f(x)$. $\mathbf{1}_N = [\underbrace{1, 1, \ldots, 1}_{N}]^T$ and I_n denotes the n-th order identity matrix.

Definition 1. *Consider the system $\dot{x}(t) = f(x(t)), x(t) \in \mathbb{R}^n$. The equilibrium point $x = 0$ is said to be exponentially stable if there exist positive constants k and λ such that for initial condition $x(t_0) \in \mathbb{R}^n$, the solution satisfies*

$$\|x(t)\| \leq ke^{-\lambda(t-t_0)}\|x(t_0)\|, \quad \forall t \geq t_0.$$

Definition 2. *$x(t) \in \mathbb{R}^n$ is said to be bounded if there exists a constant $B > 0$ such that*

$$\|x(t)\| \leq B, \quad \forall t \geq t_0.$$

2.1. Graph theory

An undirected graph $\mathcal{G} = (\mathcal{V}, \mathcal{E}, \mathcal{A})$ is applied to present the interactions among agents, in which $\mathcal{V} = \{1, \ldots, N\}$, $\mathcal{E} \subseteq \mathcal{V} \times \mathcal{V}$, and $\mathcal{A} = [a_{ij}] \in \mathbb{R}^{N\times N}$ are the node set, the edge set, and the weighted adjacency matrix, respectively. An edge $(i, j) \in \mathcal{E}$ is an unordered pair presenting the information flow between agent i and j. In this case, $a_{ij} > 0$; otherwise, $a_{ij} = 0$. It is assumed that $a_{ii} = 0$ in this paper. If agent i can sense the information of the leader agent, then $b_i > 0$. The leader adjacency matrix is defined as $\mathcal{B} = \text{diag}\{b_1, \ldots, b_N\}$. Let the degree matrix $\mathcal{D} = \text{diag}\{d_1, \ldots, d_N\}$ with $d_i = \sum_{j=1}^{N} a_{ij}$, the Laplacian matrix $\mathcal{L} = \mathcal{D} - \mathcal{A}$, and $\mathcal{H} = \mathcal{L}+\mathcal{B}$. The graph $\mathcal{G}$ is said to be connected if there exists a path between any two agents. If graph $\mathcal{G}$ is connected, then matrix $\mathcal{H}$ is symmetric positive definite [31].

2.2. Required lemmas

In this subsection, the required lemmas for theoretical analysis are given.

Lemma 2.1. *[32] For a continuous function $f(x)$ on a compact set Ω and a specified accuracy threshold $\varepsilon > 0$, there exists an FLS $\theta^T\phi(x)$ such that*

$$\sup_{x\in\Omega} |f(x) - \theta^T\phi(x)| \leq \varepsilon, \tag{2.1}$$

where $\theta = [\theta_1, \ldots, \theta_l]^T$ is the ideal weight vector and $\phi(x) = \left[\phi_1(x), \ldots, \phi_l(x)\right]^T / \sum_{i=1}^{l} \phi_i$ is the basis function vector with $\phi_i(x)$ defined as

$$\phi_i(x) = \exp\left(\frac{-(x - \bar{y}_i)^T (x - \bar{y}_i)}{m_i^2}\right), \tag{2.2}$$

where $\bar{y}_i = \left[\bar{y}_{i1}, \ldots, \bar{y}_{il}\right]^T$ and m_i are the center vector and the width, respectively.

From Lemma 2.1, a continuous function $f(x)$ can be approximated by an FLS $\theta^{*T}\phi(x)$ as $f(x) = \theta^{*T}\phi(x) + \epsilon$, in which $\theta^* = \arg\min_{x\in\Omega}[\sup_{x\in\Omega} |f(x) - \theta^T\phi(x)|]$ is the optimal parameter vector and ϵ is the approximation error satisfying $|\epsilon| \leq \bar{\epsilon}$ with $\bar{\epsilon} > 0$ being a constant.

Lemma 2.2. *[28] For any $x \in \mathbb{R}$ and $c > 0$, one has*

$$0 \leq |x| - x\tanh\left(\frac{x}{c}\right) \leq 0.2785c. \tag{2.3}$$

Lemma 2.3. *[33](Young's inequality) For any $x, y \in \mathbb{R}$, one has*

$$xy \leq \frac{q^{c_1}}{c_1}|x|^{c_1} + \frac{1}{c_2 q^{c_2}}|y|^{c_2}, \tag{2.4}$$

where $c_1 > 1, c_2 > 1, q > 0$, and $(c_1 - 1)(c_2 - 1) = 1$.

Lemma 2.4. *[34] Given an n-dimensional matrix $W > 0$, a vector function $\varphi(t) \in \mathbb{R}^n$, and a scalar $\tau > 0$, one has*

$$-\tau \int_{t-\tau}^{t} \dot{\varphi}^T(s) W \dot{\varphi}(s) ds \leqslant -[\varphi(t) - \varphi(t-\tau)]^T W [\varphi(t) - \varphi(t-\tau)]. \tag{2.5}$$

Lemma 2.5. *[35] Given matrices $W > 0$, W_1 and W_2 with appropriate dimension, a scalar $\mu \in (0, 1)$, and a function $f(W)$ satisfying*

$$f(W) = \frac{1}{\mu}\varphi^T(t) W_1^T W W_1 \varphi(t) + \frac{1}{1-\mu}\varphi^T(t) W_2^T W W_2 \varphi(t), \tag{2.6}$$

where $\varphi(t) \in \mathbb{R}^n$ is a vector function composed of matrix blocks along with appropriate dimensional matrix S such that $[W*; S\ W] \geq 0$, one has

$$\min_{\delta \in (0,1)} f(\delta, W) \geqslant \varphi^T(t) \begin{bmatrix} W_1 \\ W_2 \end{bmatrix}^T \begin{bmatrix} W & * \\ S & W \end{bmatrix} \begin{bmatrix} W_1 \\ W_2 \end{bmatrix} \varphi(t). \tag{2.7}$$

3. Problem statement

3.1. Problem description

Consider an MAS with N following agents and a leader, in which agent i is modeled by

$$\begin{cases} \dot{x}_{iq} = x_{i,q+1} + g_{iq}\left(\bar{x}_{iq}\right) + d_{iq}(t), \\ \dot{x}_{in} = u_{iD} + g_{in}(\bar{x}_{in}) + d_{in}(t), \\ y_i = x_{i1}, \end{cases} \tag{3.1}$$

where $\bar{x}_{iq} = [x_{i1}, \ldots, x_{iq}]^T \in \mathbb{R}^q, q = 1, 2, ..., n$, and let $x_i = [x_{i1}, \ldots, x_{in}]^T \in \mathbb{R}^n$ be the full state vector. $y_i \in \mathbb{R}$ is the system output. $g_{iq}(\bar{x}_{iq})$ is the uncertain nonlinear dynamics, and $d_{iq}(t) \in \mathbb{R}$ is the external disturbance satisfying $d_{iq}(t) \leq \bar{d}_{iq}$ with $\bar{d}_{iq} > 0$ being a constant. $u_{iD} \in \mathbb{R}$ is the systems input with asymmetric dead-zone nonlinearity expressed as

$$u_{iD} = \begin{cases} q_{ir}(u_i - b_{ir}), & \text{if } u_i \geq b_{ir}, \\ 0, & \text{if } -b_{il} < u_i < b_{ir}, \\ q_{il}(u_i + b_{il}), & \text{if } u_i \leq -b_{il}, \end{cases} \tag{3.2}$$

where q_{ir}, q_{il}, b_{il}, and b_{ir} are unknown positive dead-zone parameters. According to [28] and [36], the dead-zone nonlinear operator (3.2) can be rewritten as

$$u_{iD} = q_i(t)u_i(t) + p_i(t) \tag{3.3}$$

with

$$q_i(t) = \begin{cases} q_{ir}, & u_i > 0, \\ q_{il}, & u_i \le 0, \end{cases} \text{ and } p_i(t) = \begin{cases} -q_{ir}b_{ir}, & u_i \ge b_{ir}, \\ -q_i(t)u_i(t), & -b_{il} < u_i < b_{ir}, \\ q_{il}b_{il}, & u_i \le -b_{i,l}, \end{cases} \tag{3.4}$$

where $|p_i(t)| \le \bar{p}_i$ with $\bar{p}_i = \max\{q_{il}b_{il}, q_{ir}b_{ir}\}$ being a constant. Let $\underline{q_i} = \min\{q_{il}, q_{ir}\}$ and $\bar{q}_i = \max\{q_{il}, q_{ir}\}$, thus $\frac{q_i(t)}{\underline{q_i}} = 1 + \rho_i(t)$, where $\rho_i(t) > 0$ is some bounded piecewise function. It can be obtained that $0 < \rho_i \le \frac{\bar{q}_i}{\underline{q_i}} - 1$ and $u_{iD} = \underline{q_i}(1 + \rho_i(t))u_i(t) + p_i(t)$.

The dynamics of the leader agent is given by

$$\begin{cases} \dot{\eta}_0 &= A\eta_0, \\ y_0 &= C\eta_0, \end{cases} \tag{3.5}$$

where $A \in \mathbb{R}^{m\times m}$ and $C \in \mathbb{R}^{1\times m}$; $\eta_0 \in \mathbb{R}^m$ and $y_0 \in \mathbb{R}$ are the state and the output of the leader dynamics, respectively.

Remark 1. *In previous research on backstepping-based tracking control, the leader agent is typically specified as a reference signal $y(t)$ with high-order derivatives. In recent years, some scholars have extended the leader dynamics to a linear system with high-order dynamic characteristics [9, 24, 25], namely the system given by* (3.5)*, and carried out relevant research on its output tracking problem. For subsequent research, the tracking control problem where the leader has more complex nonlinear dynamics can be further investigated.*

Due to the deception attack, the actual measurement output $\check{x}_{i1}$ is given by

$$\check{x}_{i1} = x_{i1} + \omega(t, x_{i1}) = w_{i1}(t)x_{i1}, \tag{3.6}$$

where $\omega(t, x_{i1}) = s_{i1}(t)x_{i1}$ and $w_{i1}(t) = 1 + s_{i1}(t)$ with $s_{i1}(t)$ being a time-varying sensor attack signal. To facilitate the theory analysis, the following assumptions are required.

Assumption 3.1. *The graph $\mathcal{G}$ is connected, and the leader can transmit information to at least one agent.*

Assumption 3.2. *The state η_0 of the leader is bounded.*

Assumption 3.3. *[8] The attack signal $s_{i1} \ne -1$, i.e., $w_{i1} \ne 0$. s_{i1}, w_{i1}, and $\dot{w}_{i1}$ are bounded, that is, there exist positive constants $\bar{s}_{i1}$, $\bar{w}_{i1}, \underline{w}_{i1}$, and $\bar{w}_{i2}$ such that $s_{i1} \le \bar{s}_{i1}$, $\underline{w}_{i1} \le |w_{i1}| \le \bar{w}_{i1}$, and $|\dot{w}_{i1}| \le \bar{w}_{i2}$.*

Assumption 3.4. *[28] There exists an unknown constant $\bar{u}_i > 0$ such that $|u_i| \le \bar{u}_i$.*

3.2. DoS *attack*

Let $\{t_p, p \in \mathbb{N}\}$ be the time sequence of DoS attacks, where t_p is the start instant of the DoS attack. The pth DoS attack interval is defined as $[t_p, t_p + \Delta_p)$ with Δ_p being the duration of the DoS attack and $t_{p+1} > t_p + \Delta_p$. We assume that the intervals of DoS attacks are identical for all agents. The union of DoS attack intervals in $[t_0, t)$ is denoted by $\Gamma_D(t_0, t) = [t_0, t] \cap \left\{ \bigcup_{p\in\mathbb{N}}[t_p, t_p + \Delta_p)\right\}$. The time intervals without the DoS attack are denoted by $\Gamma_N(t_0, t) = [t_0, t]/\Gamma_D(t_0, t)$. If $t \in \Gamma_D(t_0, t)$, then $\bar{a}_{ij} = 0$ and $\bar{b}_i = 0$; otherwise, $\bar{a}_{ij} = a_{ij}$ and $\bar{b}_i = b_i$.

Assumption 3.5. *[24] There exist two constants $\Gamma_0 \geq 0$ and $\Gamma_1 \geq 1$ such that $|\Gamma_D(t_0, t)| \leqslant \Gamma_0 + t/\Gamma_1$, where $|\Gamma_D(t_0, t)|$ represents the total duration of DoS attacks on the communication network in $[t_0, t)$.*

Assumption 3.6. *[37] Let $\Pi_D(t_0, t)$ be the total number of DoS attacks on the communication network in $[t_0, t]$. The attack frequency $\Pi_D(t_0, t)$ satisfies $|\Pi_D(t_0, t)| \leq \Pi_0 + (t - t_0)/\Pi_1$, where Π_0 and Π_1 are two positive constants.*

Assumption 3.5 indicates that attackers are unable to sustain an extended attack, whereas Assumption 3.6 limits the frequency of DoS attacks within a specific time period. It is worth emphasizing that an additional time interval $\Delta_*(\Delta_* \leq \tau_p)$ is required to resume normal communication following DoS attacks. As such, the effective duration of a DoS attack interval proves longer than the duration that is reported. Consequently, the total actual duration of DoS attack intervals within $[t_0, t]$ may be calculated as follows:

$$\tilde{\Gamma}_D(t_0, t) = [t_0, t] \cap \left\{ \bigcup_{p\in\mathbb{N}} [t_p, t_p + \Delta_p + \Delta_*)\right\}. \tag{3.7}$$

4. Distributed leader state estimator and filter design

4.1. Distributed leader state estimator design

In this section, a distributed state estimator of the leader agent is designed. For agent i, let η_i be the estimation of the leader state η_0. In the presence of DoS attacks, a distributed state estimator is constructed using sampling data with time delays as follows:

$$\dot{\eta}_i = A\eta_i - \gamma K_i \sum_{j=1}^{N} \bar{a}_{ij}[\eta_i(kh) - \eta_j(kh)] - \gamma K_i \bar{b}_i \left[\eta_i(kh) - \eta_0(kh)\right], \tag{4.1}$$

where $\gamma > 0$ is a design parameter, K_i is the gain matrix, which will be designed later, h is the sampling period, and $k = 1, 2, \cdots$.

Let $\tau(t) = t - kh$ for $t \in [\tau_k + kh, \tau_{k+1} + (k + 1)h]$ be an artificial time delay, where τ_k is the kth delay. Thus, $\eta_i(kh) = \eta_i(t - \tau(t))$. It can be observed that $\tau_k \leqslant \tau(t) \leqslant \tau_{k+1} + h$. Let $\underline{\tau} = \min_{k=1,\ldots,\infty} \tau_k$, $\bar{\tau} = h + \max_{k=1,\ldots,\infty} \tau_k$, and $\tilde{\tau} = \bar{\tau} - \underline{\tau}$. Thus, $0 \leqslant \underline{\tau} \leqslant \tau(t) \leqslant \bar{\tau}$.

According to the above settings, (4.1) can be rewritten as

$$\dot{\eta}_i = A\eta_i - \gamma K_i \sum_{j=1}^{N} \bar{a}_{ij}[\eta_i(t - \tau(t)) - \eta_j(t - \tau(t))]$$

$$- \gamma K_i \bar{b}_i \left(\eta_i(t-\tau(t)) - \eta_0(t-\tau(t))\right). \tag{4.2}$$

Let $\bar{\eta}_i = \eta_i - \eta_0$ be the estimation error for agent i, $\eta = [\eta_1, \ldots, \eta_N]^T$, and $\bar{\eta} = \eta - \mathbf{1}_N \eta_0$. The dynamics of estimation error under the influence of DoS attacks and time delays can be rephrased as

$$\dot{\bar{\eta}} = \begin{cases} (I_N \otimes A)\bar{\eta}(t) - \gamma K (\mathcal{H} \otimes I_n)\bar{\eta}(t-\tau(t)), & t \in \Gamma_N(t_0, t), \\ (I_N \otimes A)\bar{\eta}(t), & t \in \Gamma_D(t_0, t), \end{cases} \tag{4.3}$$

where $K = \mathrm{diag}\{K_1, K_2, \ldots, K_N\}$.

Theorem 4.1. *Under Assumptions 3.1, 3.5, and 3.6, for given positive constants a and b, the error system* (4.3) *is exponentially stable if there exist positive definite $Nn \times Nn$ matrices Q_1, Q_2, Z_1, Z_2 and P and a matrix $S \in \mathbb{R}^{Nn \times Nn}$ such that $\Phi < 0$, $\Psi < 0$, and $-a + \frac{a+b}{\Gamma_1} + \frac{(a+b)\Delta_*}{\Pi_1} < 0$ hold, where Φ and Ψ are given in Appendix A.*

Proof: Construct the Lyapunov functional candidate as

$$\begin{aligned} V_1 =& \bar{\eta}^T(t) P \bar{\eta}(t) + \int_{t-\underline{\tau}}^{t} e^{a(s-t)} \bar{\eta}^T(s) Q_1 \bar{\eta}(s) ds \\ &+ \int_{t-\bar{\tau}}^{t-\underline{\tau}} e^{a(s-t)} \bar{\eta}^T(s) Q_2 \bar{\eta}(s) ds \\ &+ \underline{\tau} \int_{-\underline{\tau}}^{0} \int_{t+\theta}^{t} e^{a(s-t)} \dot{\bar{\eta}}^T(s) Z_1 \dot{\bar{\eta}}(s) ds d\theta \\ &+ \tilde{\tau} \int_{-\bar{\tau}}^{-\underline{\tau}} \int_{t+\theta}^{t} e^{a(s-t)} \dot{\bar{\eta}}^T(s) Z_2 \dot{\bar{\eta}}(s) ds d\theta. \end{aligned} \tag{4.4}$$

The proof is divided into the following three cases:

Case 1: For $t \in \Gamma_N(t_0, t)$, the derivative of $V_1(t)$ is calculated as

$$\begin{aligned} \dot{V}_1 =& - aV_1 + \bar{\eta}^T(t) \left\{ P(I_N \otimes A) + (I_N \otimes A)^T P + aP \right\} \bar{\eta}(t) \\ &+ \bar{\eta}^T(t) Q_1 \bar{\eta}(t) - 2\gamma \bar{\eta}^T(t) PK(\mathcal{H} \otimes I_n) \bar{\eta}(t-\tau(t)) \\ &+ e^{-a\underline{\tau}} \bar{\eta}^T(t-\underline{\tau})(Q_2 - Q_1) \bar{\eta}^T(t-\underline{\tau}) - e^{-a\bar{\tau}} \bar{\eta}^T(t-\bar{\tau}) Q_2 \bar{\eta}(t-\bar{\tau}) \\ &+ \dot{\bar{\eta}}^T(t)(\underline{\tau}^2 Z_1 + \tilde{\tau}^2 Z_2) \dot{\bar{\eta}}(t) - \underline{\tau} \int_{t-\underline{\tau}}^{t} e^{a(s-t)} \dot{\bar{\eta}}^T(s) Z_1 \dot{\bar{\eta}}(s) ds \\ &- \tilde{\tau} \int_{t-\bar{\tau}}^{t-\underline{\tau}} e^{a(s-t)} \dot{\bar{\eta}}^T(s) Z_2 \dot{\bar{\eta}}(s) ds \\ =& - aV_1 + \tilde{\eta}^T(t) \delta_1^T \left\{ P(I_N \otimes A) + (I_N \otimes A)^T P + aP \right\} \delta_1 \tilde{\eta}(t) \\ &+ \tilde{\eta}^T(t) \delta_1^T Q_1 \delta_1 \tilde{\eta}(t) - 2\gamma \tilde{\eta}^T(t) \delta_1^T PK(\mathcal{H} \otimes I_n) \delta_2 \tilde{\eta}(t) \\ &+ e^{-a\underline{\tau}} \tilde{\eta}^T(t) \delta_3^T (Q_2 - Q_1) \delta_3 \tilde{\eta}(t) - e^{-a\bar{\tau}} \tilde{\eta}^T(t) \delta_4^T Q_2 \delta_4 \tilde{\eta}(t) \\ &- \underline{\tau} \int_{t-\underline{\tau}}^{t} e^{a(s-t)} \dot{\bar{\eta}}^T(s) Z_1 \dot{\bar{\eta}}(s) ds - \tilde{\tau} \int_{t-\bar{\tau}}^{t-\underline{\tau}} e^{a(s-t)} \dot{\bar{\eta}}^T(s) Z_2 \dot{\bar{\eta}}(s) ds \\ &+ \dot{\bar{\eta}}^T(t)(\underline{\tau}^2 Z_1 + \tilde{\tau}^2 Z_2) \dot{\bar{\eta}}(t), \end{aligned} \tag{4.5}$$

where $\tilde{\eta}(t) = \left[\bar{\eta}^T(t), \bar{\eta}^T(t-\tau(t)), \bar{\eta}^T(t-\underline{\tau}), \bar{\eta}^T(t-\bar{\tau})\right]^T$. δ_i $(i = 1, \ldots, 4)$ is defined as a block entry matrix, and $\delta_{ij} = \delta_i - \delta_j$, for instance, $\delta_1 = [I_{Nn}, 0, 0, 0]$, $\delta_2 = [0, I_{Nn}, 0, 0]$, and $\delta_{12} = [I_{Nn}, -I_{Nn}, 0, 0]$.

Based on Lemmas 2.4 and 2.5, one obtains that

$$-\underline{\tau}\int_{t-\underline{\tau}}^{t} e^{a(s-t)}\dot{\bar{\eta}}_i^T(s)Z_1\dot{\bar{\eta}}_i(s)ds \leq -e^{-a\underline{\tau}}\tilde{\eta}^T(t)\delta_{13}^T Z_1\delta_{13}\tilde{\eta}(t) \tag{4.6}$$

and

$$\begin{aligned}
&-\tilde{\tau}\int_{t-\bar{\tau}}^{t-\underline{\tau}} e^{a(s-t)}\dot{\bar{\eta}}_i^T(s)Z_2\dot{\bar{\eta}}_i(s)ds \\
&\leq -\frac{\tilde{\tau}e^{-a\bar{\tau}}}{\bar{\tau}-\tau(t)}\tilde{\eta}^T(t)\delta_{24}^T Z_2\delta_{24}\tilde{\eta}(t) - \frac{\tilde{\tau}e^{-a\bar{\tau}}}{\tau(t)-\underline{\tau}}\tilde{\eta}^T(t)\delta_{32}^T Z_2\delta_{32}\tilde{\eta}(t) \\
&\leq -e^{-a\bar{\tau}}\tilde{\eta}^T(t)\begin{bmatrix}\delta_{24}\\ \delta_{32}\end{bmatrix}^T\begin{bmatrix}Z_2 & S\\ S^T & Z_2\end{bmatrix}\begin{bmatrix}\delta_{24}\\ \delta_{32}\end{bmatrix}\tilde{\eta}(t).
\end{aligned} \tag{4.7}$$

From (4.5)–(4.7), applying the Schur complement lemma derives that

$$\dot{V}_1(t) \leq -aV_1(t) + \tilde{\eta}^T(t)\Phi\tilde{\eta}(t). \tag{4.8}$$

It is clear that if $\Phi < 0$, then $V_1(t) \leqslant e^{-a(t-t_0)}V_1(t_0)$.

Case 2: For $t \in \Gamma_D(t_0, t)$, similar to the case without DoS attacks in (4.5), substituting $-b$ for a yields that

$$\begin{aligned}
\dot{V}_1 =& bV_1 + \tilde{\eta}^T(t)\delta_1^T\left[P(I_N\otimes A) + (I_N\otimes A)^T P - bP\right]\delta_1\tilde{\eta}(t) + \tilde{\eta}^T(t)\delta_1^T Q_1\delta_1\tilde{\eta}(t) \\
&+ e^{b\underline{\tau}}\tilde{\eta}^T(t)\delta_3^T(Q_2-Q_1)\delta_3\tilde{\eta}(t) - e^{b\bar{\tau}}\tilde{\eta}(t)^T\delta_4^T Q_2\delta_4\tilde{\eta}(t) \\
&- \underline{\tau}\int_{t-\underline{\tau}}^{t} e^{-b(s-t)}\dot{\bar{\eta}}^T(s)Z_1\dot{\bar{\eta}}(s)ds - \tilde{\tau}\int_{t-\bar{\tau}}^{t-\underline{\tau}} e^{-b(s-t)}\dot{\bar{\eta}}^T(s)Z_2\dot{\bar{\eta}}(s)ds \\
&+ \dot{\bar{\eta}}^T(t)(\underline{\tau}^2 Z_1 + \tilde{\tau}^2 Z_2)\dot{\bar{\eta}}(t).
\end{aligned} \tag{4.9}$$

Applying the Schur complement lemma yields that

$$\dot{V}_1(t) \leq bV_1(t) + \tilde{\eta}^T(t)\Psi\tilde{\eta}(t). \tag{4.10}$$

It is clear that if $\Psi < 0$, then $V_1(t) \leqslant e^{b(t-t_0)}V_1(t_0)$.

Case 3: We take into account two potential scenarios of DoS attacks in the time domain. Defining $[t_{n-1} + \Delta_{n-1}, t_n) \triangleq T_{n1}$ and $[t_n, t_n + \Delta_n] \triangleq T_{n2}$, and according to (4.8) and (4.10), one obtains that

$$\begin{cases} V_1(t) \leqslant e^{-a(t-t_{n-1}-\Delta_{n-1})}V_1\left(t_{n-1}+\Delta_{n-1}\right), & t \in T_{n1}, \\ V_1(t) \leqslant e^{b(t-t_n)}V_1\left(t_n\right), & t \in T_{n2}. \end{cases} \tag{4.11}$$

From (4.11) and Assumption 3.5, if $t \in T_{n1}$, we get

$$V_1(t) \leq e^{-a\left|\tilde{\Gamma}_N(t_0,t)\right|}e^{b\left|\tilde{\Gamma}_D(t_0,t)\right|}V_1(t_0). \tag{4.12}$$

Similarly, if $t \in T_{n2}$, one has

$$\begin{aligned} V_1(t) &\leq e^{b(t-t_n)} V_1(t_n) \\ &\leq e^{b(t-t_n)} e^{-a(t_n - t_{n-1} - \Delta_{n-1})} V_1(t_{n-1} + \Delta_{n-1}) \\ &\leq \cdots \leqslant e^{-a\left|\tilde{\Gamma}_N(t_0,t)\right|} e^{b\left|\tilde{\Gamma}_D(t_0,t)\right|} V_1(t_0). \end{aligned} \tag{4.13}$$

Based on (4.12) and (4.13), under Assumption 3.5 and 3.6, we have

$$\begin{aligned} & e^{-a\left|\tilde{\Gamma}_N(t_0,t)\right|} e^{b\left|\tilde{\Gamma}_D(t_0,t)\right|} \\ &= e^{-a\left(t-t_0-\left|\tilde{\Gamma}_D(t_0,t)\right|\right)} e^{b\left|\tilde{\Gamma}_D(t_0,t)\right|} \\ &\leqslant e^{-a(t-t_0)} e^{(a+b)\left(\Gamma_0 + \frac{t-t_0}{\Gamma_1} + (\Pi_0 + \frac{t-t_0}{\Pi_1} + 1)\Delta_*\right)} \\ &\leqslant e^{(a+b)(\Gamma_0 + (1+\Pi_0)\Delta_*)} e^{(t-t_0)\left(-a + \frac{a+b}{\Gamma_1} + \frac{(a+b)\Delta_*}{\Pi_1}\right)}. \end{aligned} \tag{4.14}$$

From (4.12)–(4.14), we can deduce that $\lim_{t\to\infty} V_1(t) = 0$ under the aforementioned DoS attack scenarios, which implies that $\bar{\eta}_i$ converges exponentially to zero. This completes the proof.

Remark 2. *The quantitative relationship between the attack intensity and the linear matrix inequality (LMI) feasibility is characterized by the condition* $-a + \frac{a+b}{\Gamma_1} + \frac{(a+b)\Delta_*}{\Pi_1} < 0$ *given in Theorem 4.1. Here, the attack intensity is captured by two DoS attack parameters* Γ_1 *and* Π_1*. The design parameters a and b correspond to the convergence rates of the Lyapunov function during attack-free periods and under DoS attacks, respectively. When the combined attack duration and frequency—which are inversely related to* Γ_1 *and* Π_1 *—exceed a certain level, the inequality condition fails and the LMIs in Theorems 4.1 and 4.2 become infeasible. Due to the coupling relationship between parameters* Γ_1 *and* Π_1 *in the inequality, it is difficult to obtain the maximum tolerable attack intensity. However, the inequality condition offers an effective design guideline: For given attack parameters* Γ_1 *and* Π_1*, one can adjust the convergence rate parameters a and b such that the inequality condition holds.*

In Theorem 4.1, due to the existence of matrices PK, $\alpha^2 Z_1 + \tilde{\tau}^2 Z_2$, and its inverse matrix, the matrix inequalities $\Phi < 0$ and $\Psi < 0$ do not have linear forms. By multiplying both sides of matrices Φ and Ψ by $X = \text{diag}\{I_{Nn}, I_{Nn}, I_{Nn}, I_{Nn}, P\}$, setting $P = K^{-1}$, and applying the inequality $-P(\underline{\tau}^2 Z_1 + \tilde{\tau}^2 Z_2)^{-1} P \leq \mu^2(\underline{\tau}^2 Z_1 + \tilde{\tau}^2 Z_2) - 2\mu P$ with $\mu > 0$ being a constant, the matrix inequalities $\Phi < 0$ and $\Psi < 0$ can be converted into LMIs, as stated in the following theorem.

Theorem 4.2. *Suppose that Theorem 4.1 is satisfied. For a given positive constant* μ*, one has* $\tilde{\Phi} < 0$ *and* $\tilde{\Psi} < 0$*, where* $\tilde{\Phi}$ *and* $\tilde{\Psi}$ *are given in Appendix B.*

4.2. Filter design

Affected by the combined influence of DoS attacks and sampled data, the high-order derivatives of $\eta_i(t)$ do not exist at switching instants, and this problem hinders the smooth implementation of the backstepping method. Drawing on the idea of [37], this paper proposes the following filter to estimate the 2^{nd} to nth derivatives of $\eta_i(t)$.

Define a variable ξ_{i1} to represent the estimation of η_i, where ξ_{i1} admits derivatives up to the nth order, specified as

$$\dot{\xi}_{i1} = A\xi_{i1} - \sigma(\xi_{i1} - \xi_{i2}),$$

$$\dot{\xi}_{i2} = A\xi_{i2} - \sigma(\xi_{i2} - \xi_{i3}),$$
$$\cdots$$
$$\dot{\xi}_{i,n-1} = A\xi_{i,n-1} - \sigma\bar{\xi}_{i,n-1}, \tag{4.15}$$

where $\bar{\xi}_{i,n-1} = \xi_{i,n-1} - \eta_i$ and $\sigma > 0$ is a design parameter satisfying $A - \sigma I < 0$.

From (4.2) and (4.15), one obtains that

$$\dot{\bar{\xi}}_{i,n-1} = (A - \sigma I)\bar{\xi}_{i,n-1} + \gamma K_i \sum_{j=1}^{N} \bar{a}_{ij}[\bar{\eta}_i(t - \tau(t)) - \bar{\eta}_j(t - \tau(t))]$$
$$+ \gamma K_i \bar{b}_i \bar{\eta}_i(t - \tau(t)). \tag{4.16}$$

It follows from $A - \sigma I < 0$ and the exponential convergence of $\bar{\eta}_i$ that $\bar{\xi}_{i,n-1}$ converges to zero exponentially.

Let $\tilde{\xi}_{i1} = \xi_{i1} - \xi_{i2}$, $\tilde{\xi}_{i2} = \xi_{i2} - \xi_{i3}$, …, $\tilde{\xi}_{i,n-2} = \xi_{i,n-2} - \xi_{i,n-1}$. From (4.15), we have

$$\dot{\tilde{\xi}}_{i1} = (A - \sigma I)\tilde{\xi}_{i1} + \sigma\tilde{\xi}_{i2},$$
$$\dot{\tilde{\xi}}_{i2} = (A - \sigma I)\tilde{\xi}_{i2} + \sigma\tilde{\xi}_{i3},$$
$$\cdots$$
$$\dot{\tilde{\xi}}_{i,n-2} = (A - \sigma I)\tilde{\xi}_{i,n-2} + \sigma\bar{\xi}_{i,n-1}. \tag{4.17}$$

It follows from the exponential convergence of $\bar{\xi}_{i,n-1}$ that $\tilde{\xi}_{i1}, \tilde{\xi}_{i2}, \ldots,$ and $\tilde{\xi}_{i,n-2}$ also converge to zero exponentially.

Remark 3. *The design idea of filter* (4.17) *is borrowed from [25], where the filter parameters are required to be Hurwitz coefficients. Unlike [25], the filter parameter in this paper only needs to be set as a positive design parameter.*

5. State observer design

A state observer is constructed as follows:

$$\begin{cases} \dot{\hat{x}}_{iq} = \hat{x}_{i,q+1} + l_{iq}\,(\breve{x}_{i1} - \hat{x}_{i1})\ \ q = 1, \ldots, n-1, \\ \dot{\hat{x}}_{in} = u_{iD} + l_{in}\,(\breve{x}_{i1} - \hat{x}_{i1})\,, \\ \hat{y}_i = \hat{x}_{i1}, \end{cases} \tag{5.1}$$

where $\hat{x}_{iq}, q = 1, 2, \ldots, n$ are the states of the observer for agent i and $l_{iq} > 0, q = 1, 2, \ldots, n$ are design parameters. Let $\hat{\bar{x}}_{iq} = [\hat{x}_{i1}, \ldots, \hat{x}_{iq}]^T$ and $\hat{x}_i = [\hat{x}_{i1}, \ldots, \hat{x}_{in}]^T$ be the full state vector.

Define the observer error $e_i = x_i - \hat{x}_i = [e_{i1}, \ldots, e_{in}]^T$, and one has

$$\dot{e}_i = A_i e_i + g_i + d_i - l_i\omega_s, \tag{5.2}$$

where $A_i = \begin{bmatrix} -l_{i1} & 1 & 0 & \cdots & 0 \\ -l_{i2} & 0 & 1 & \cdots & 0 \\ \vdots & \vdots & \vdots & \cdots & \vdots \\ -l_{i,n-1} & 0 & 0 & \cdots & 1 \\ -l_{in} & 0 & 0 & \cdots & 0 \end{bmatrix}$, $g_i = \begin{bmatrix} g_{i1}(x_{i1}) \\ g_{i2}(\bar{x}_{i2}) \\ \vdots \\ g_{in}(\bar{x}_{in}) \end{bmatrix}$, $l_i = \begin{bmatrix} l_{i1} \\ l_{i2} \\ \vdots \\ l_{in} \end{bmatrix}$, $d_i = \begin{bmatrix} d_{i1} \\ d_{i2} \\ \vdots \\ d_{in} \end{bmatrix}$, and $\|d_i\| \le \bar{d}_i$ with $\bar{d}_i$ being a constant.

Select the vector l_i to ensure that A_i is Hurwitz, so for a given matrix $Q_i > 0$, there exists a positive definite matrix P_i such that $A_i^T P_i + P_i A_i = -Q_i$.

Define the Lyapunov function V_0 as

$$V_0 = \sum_{i=1}^{n} V_{i0} = \sum_{i=1}^{n} \frac{1}{a_i} e_i^T P_i e_i, \tag{5.3}$$

where $a_i = \|P_i\|\|l_i\|\bar{s}_{i1}\underline{w}_{i1}^{-1}$.

Its time derivative is

$$\begin{aligned}\dot{V}_{i0} =& -\frac{1}{a_i} e_i^T Q_i e_i + \frac{2}{a_i} e_i^T P_i (g_i + d_i - l_i\omega_s)\\ =& -\frac{1}{a_i} e_i^T Q_i e_i + \frac{2}{a_i} e_i^T P_i (g_i + d_i) - \frac{2}{a_i} e_i^T P_i l_i \omega_s.\end{aligned} \tag{5.4}$$

According to Lemma 2.3, it derives that

$$\frac{2}{a_i} e_i^T P_i (g_i + d_i) \le 2\tau_{i0}^{(1)}\|e_i\|^2 + \frac{\underline{w}_{i1}^2}{\tau_{i0}^{(1)}\|l_i\|^2\bar{s}_{i1}^2}\|g_i\|^2 + \frac{\underline{w}_{i1}^2}{\tau_{i0}^{(1)}\|l_i\|^2\bar{s}_{i1}^2}\bar{d}_i^2, \tag{5.5}$$

where $\tau_{i0}^{(1)} > 0$ is a constant.

For the unknown nonlinear term $\frac{\underline{w}_{i1}^2}{\|l_i\|^2\bar{s}_{i1}^2}\|g_i\|^2$ in (5.5), according to Lemma 2.1, an FLS $\theta_{i0}^T\varphi_{i0}$ is utilized such that $\frac{\underline{w}_{i1}^2}{\|l_i\|^2\bar{s}_{i1}^2}\|g_i\|^2 = \theta_{i0}^T\phi_{i0}(\bar{x}_{in}) + \epsilon_{i0}$, where $\bar{x}_{in} = [x_{i1}, \ldots, x_{in}]^T$ and ϵ_{i0} is the approximation error satisfying $|\epsilon_{i0}| \le \bar{\epsilon}_{i0}$. With the fact that $0 < \phi_{i0}^T\phi_{i0} \le 1$, one has $\frac{\underline{w}_{i1}^2}{\|l_i\|^2\bar{s}_{i1}^2}\|g_i\|^2 \le \|\theta_{i0}\|\|\phi_{i0}\| + |\epsilon_{i0}| \le \vartheta_{i0} + \bar{\epsilon}_{i0}$, where $\vartheta_{i0} = \|\theta_{i0}\|$.

Thus,

$$\begin{aligned}\dot{V}_{i0} \le& -\frac{1}{a_i} e_i^T Q_i e_i + 2\tau_{i0}^{(1)}\|e_i\|^2 + \frac{\underline{w}_{i1}^2}{\tau_{i0}^{(1)}\|l_i\|^2\bar{s}_{i1}^2}\bar{d}_i^2 + \frac{1}{\tau_{i0}^{(1)}}(\vartheta_{i0} + \bar{\epsilon}_{i0})\\ & - \frac{2}{a_i} e_i^T P_i l_i \omega_s\\ \le& -c_{i0}^{(0)} e_i^T e_i - \frac{2}{a_i} e_i^T P_i l_i \omega_s + M_{i0},\end{aligned} \tag{5.6}$$

where $c_{i0}^{(0)} = \frac{1}{a_i}\lambda_{\min}(Q_i) - 2\tau_{i0}^{(1)}$ and $M_{i0} = \frac{1}{\tau_{i0}^{(1)}}(\vartheta_{i0} + \bar{\epsilon}_{i0}) + \frac{\underline{w}_{i1}^2}{\tau_{i0}^{(1)}\|l_i\|^2\bar{s}_{i1}^2}\bar{d}_i^2$.

6. Adaptive control design

Define the following coordinate transformation:

$$\begin{aligned} z_{i1} &= \breve{x}_{i1} - C\xi_{i1},\\ z_{iq} &= \hat{x}_{iq} - \alpha_{i,q-1},\ q = 2, \ldots, n,\end{aligned} \tag{6.1}$$

where $\alpha_{i,q-1}$ is the virtual controller.

The adaptive backstepping design procedure is presented as follows:

Step 1: From (3.1) and (3.6), one gets

$$\begin{aligned}\dot{z}_{i1} =&\dot{\bar{x}}_{i1} - C\dot{\xi}_{i1}\\ =&\dot{w}_{i1}x_{i1} + w_{i1}\left(z_{i2} + \alpha_{i1} + e_{i2} + g_{i1}(\bar{x}_{i1}) + d_{i1}\right) - C\dot{\xi}_{i1}.\end{aligned} \tag{6.2}$$

Construct the Lyapunov function V_{i1} as

$$V_{i1} = V_{i0} + \frac{1}{2}z_{i1}^2 + \frac{1}{2\underline{w}_{i1}}\tilde{\vartheta}_{i1}^2, \tag{6.3}$$

where $\tilde{\vartheta}_{i1} = \vartheta_{i1} - \underline{w}_{i1}\hat{\vartheta}_{i1}$ and $\hat{\vartheta}_{i1}$ is the estimation of ϑ_{i1}. The definition of ϑ_{i1} will be given later.

Its time derivative is calculated as

$$\begin{aligned}\dot{V}_{i1} =&\dot{V}_{i0} + z_{i1}\dot{z}_{i1} - \tilde{\vartheta}_{i1}\dot{\hat{\vartheta}}_{i1}\\ =&-c_{i0}^{(0)}e_i^Te_i - \frac{2}{a_i}e_i^TP_il_i\omega_s + z_{i1}\Big[\dot{w}_{i1}x_{i1} + w_{i1}\left(z_{i2} + \alpha_{i1} + e_{i2} + g_{i1}(\bar{x}_{i1})\right.\\ &\left.+d_{i1}\right) - C\dot{\xi}_{i1}\Big] - \tilde{\vartheta}_{i1}\dot{\hat{\vartheta}}_{i1} + M_{i0}\\ =&-c_{i0}^{(0)}e_i^Te_i + z_{i1}\dot{w}_{i1}\left(e_{i1} + \hat{x}_{i1}\right) + z_{i1}\Big[w_{i1}\left(z_{i2} + \alpha_{i1} + e_{i2} + g_{i1}(\bar{x}_{i1})\right.\\ &\left.+d_{i1}\right) - C\dot{\xi}_{i1}\Big] - \tilde{\vartheta}_{i1}\dot{\hat{\vartheta}}_{i1} - \frac{2}{a_i}e_i^TP_il_is_{i1}w_{i1}^{-1}\left(z_{i1} + C\xi_{i1}\right) + M_{i0}.\end{aligned} \tag{6.4}$$

Using Lemma 2.3, one has

$$z_{i1}\dot{w}_{i1}e_{i1} \le \tau_{i1}^{(1)}\|e_i\|^2 + \frac{1}{4\tau_{i1}^{(1)}}\bar{w}_{i2}^2z_{i1}^2, \tag{6.5}$$

$$z_{i1}\dot{w}_{i1}\hat{x}_{i1} \le z_{i1}\bar{w}_{i2}\hat{x}_{i1}\tanh(\frac{z_{i1}\bar{w}_{i2}\hat{x}_{i1}}{\tau_{i1}^{(2)}}) + 0.2785\tau_{i1}^{(2)}, \tag{6.6}$$

$$-\frac{2}{a_i}e_i^TP_il_is_{i1}w_{i1}^{-1}\left(z_{i1} + C\xi_{i1}\right) \le 2\|e_i\|^2 + \frac{1}{\tau_{i1}^{(2)}}z_{i1}^2 + \frac{1}{\tau_{i1}^{(2)}}\varepsilon_{i1}, \tag{6.7}$$

$$z_{i1}w_{i1}\left(z_{i2} + e_{i2}\right) \le \tau_{i1}^{(3)}\|e_i\|^2 + \tau_{i1}^{(3)}z_{i2}^2 + \frac{1}{2\tau_{i1}^{(3)}}\bar{w}_{i1}^2z_{i1}^2, \tag{6.8}$$

and

$$z_{i1}w_{i1}d_{i1} \le \tau_{i1}^{(4)}\bar{d}_{i1}^2 + \frac{1}{2\tau_{i1}^{(4)}}\bar{w}_{i1}^2z_{i1}^2, \tag{6.9}$$

where $\|C\xi_{i1}\|^2 \le \varepsilon_{i1}$, and ε_{i1} and $\tau_{i1}^{(l)}$ for $l = 1, 2, \ldots, 4$ are positive constants.

Let

$$G_{i1}(X_{i1}) =\Big(\frac{1}{4\tau_{i1}^{(1)}}\bar{w}_{i2}^2 + \frac{1}{\tau_{i1}^{(2)}} + \frac{1}{2\tau_{i1}^{(3)}}\bar{w}_{i1}^2 + \frac{1}{2\tau_{i1}^{(4)}}\bar{w}_{i1}^2\Big)z_{i1} - C\dot{\xi}_{i1} + \bar{w}_{i2}\hat{x}_{i1}\tanh(\frac{z_{i1}\bar{w}_{i2}\hat{x}_{i1}}{\tau_{i1}^{(2)}}) + g_{i1}(\bar{x}_{i1}), \tag{6.10}$$

where $X_{i1} = [\breve{x}_{i1}, \hat{x}_{i1}, \xi_{i1}, \dot{\xi}_{i1}]^T$.

Thus,

$$\dot{V}_{i1} \leq - c_{i0}^{(1)}e_i^T e_i + z_{i1}w_{i1}\alpha_{i1} + z_{i1}G_{i1}(X_{i1}) - \tilde{\vartheta}_{i1}\dot{\hat{\vartheta}}_{i1} + \tau_{i1}^{(3)}z_{i2}^2 + M_{i0} + \tau_{i1}^{(4)}\bar{d}_{i1}^2 + \frac{1}{\tau_{i1}^{(2)}}\varepsilon_{i1} + 0.2785\tau_{i1}^{(2)}, \tag{6.11}$$

where $c_{i0}^{(1)} = c_{i0}^{(0)} - \tau_{i1}^{(1)} - \tau_{i1}^{(3)} - 2$.

Using an FLS $\theta_{i1}^T\phi_{i1}$ to approximate the unknown function G_{i1}, one gets $G_{i1} = \theta_{i1}^T\phi_{i1} + \epsilon_{i1}$, where ϵ_{i1} is the estimation error satisfying $|\epsilon_{i1}| \leq \bar{\epsilon}_{i1}$ with $\bar{\epsilon}_{i1}$ being a constant. Thus,

$$\begin{aligned} z_{i1}G_{i1} =& z_{i1}(\theta_{i1}^T\phi_{i1} + \epsilon_{i1}) \\ \leq& \vartheta_{i1}\varphi_{i1}z_{i1}\tanh(\frac{z_{i1}\varphi_{i1}}{\gamma_{i1}^{(3)}}) + 0.2875\gamma_{i1}^{(3)}\vartheta_{i1}, \end{aligned} \tag{6.12}$$

where $\vartheta_{i1} = \max\{\bar{\epsilon}_{i1}, \|\theta_{i1}\|\}$, $\varphi_{i1} = 1 + \|\phi_{i1}\|$, and $\gamma_{i1}^{(3)} > 0$ is a design parameter.

The virtual controller α_{i1} and the adaptive law $\dot{\hat{\vartheta}}_{i1}$ are designed as

$$\alpha_{i1} = -\gamma_{i1}^{(1)}z_{i1} - \hat{\vartheta}_{i1}\varphi_{i1}\tanh(\frac{z_{i1}\varphi_{i1}}{\gamma_{i1}^{(3)}}) \tag{6.13}$$

and

$$\dot{\hat{\vartheta}}_{i1} = -\gamma_{i1}^{(2)}\hat{\vartheta}_{i1} + z_{i1}\varphi_{i1}\tanh(\frac{z_{i1}\varphi_{i1}}{\gamma_{i1}^{(3)}}), \tag{6.14}$$

where $\gamma_{i1}^{(1)}, \gamma_{i1}^{(2)}$ are positive design parameters.

In accordance with (6.11)–(6.14), it can be obtained that

$$\dot{V}_{i1} \leq -c_{i0}^{(1)}e_i^T e_i - \gamma_{i1}^{(1)}z_{i1}^2 + \gamma_{i1}\tilde{\vartheta}_{i1}\hat{\vartheta}_{i1} + \tau_{i1}^{(3)}z_{i2}^2 + M_{i1}, \tag{6.15}$$

where $M_{i1} = M_{i0} + \frac{1}{\tau_{i1}^{(2)}}\varepsilon_{i1} + 0.2785\gamma_{i1}^{(3)}\vartheta_{i1} + 0.2785\tau_{i1}^{(2)} + \tau_{i1}^{(4)}\bar{d}_{i1}^2$.

Step p ($2 \leqslant p \leqslant n-1$): From (6.1), we have

$$\begin{aligned} \dot{z}_{ip} =& \dot{\hat{x}}_{i1} - \dot{\alpha}_{i,p-1} \\ =& z_{i,p+1} + \alpha_{ip} + l_{ip}(\breve{x}_{i1} - \hat{x}_{i1}) - \dot{\alpha}_{i,p-1}. \end{aligned} \tag{6.16}$$

Define the Lyapunov function V_{ip} as

$$V_{ip} = V_{i,p-1} + \frac{1}{2}z_{ip}^2 + \frac{1}{2}\tilde{\vartheta}_{ip}^2, \tag{6.17}$$

where $\tilde{\vartheta}_{ip} = \vartheta_{ip} - \hat{\vartheta}_{ip}$ and $\hat{\vartheta}_{ip}$ is the estimation of ϑ_{ip}. The definition of ϑ_{ip} will be given later.

The derivative of V_{ip} is calculated as

$$\begin{aligned}\dot{V}_{ip} =&\dot{V}_{i,p-1} + z_{ip}\dot{z}_{ip} - \tilde{\vartheta}_{ip}\dot{\hat{\vartheta}}_{ip}\\ =&- c_{i0}^{(1)} e_i^T e_i - \sum_{j=1}^{p-1}\gamma_{ij}^{(1)} z_{ij}^2 + \sum_{j=1}^{p-1}\gamma_{ij}^{(2)}\tilde{\vartheta}_{ij}\hat{\vartheta}_{ij} + \tau_{i,p-1}^{(3)} z_{ip}^2 + M_{i,p-1}\\ &+ z_{ip}\left[z_{i,p+1} + \alpha_{ip} + l_{ip}\left(w_{i1}^{-1}+1\right)(z_{i1}+C\xi_i) - \dot{\alpha}_{i,p-1}\right] - \tilde{\vartheta}_{ip}\dot{\hat{\vartheta}}_{ip}.\end{aligned} \tag{6.18}$$

Using Lemma 2.3, one has

$$l_{ip}(w_{i1}^{-1}+1)z_{ip}z_{i1} \le l_{ip}\underline{w}_{i1}^{-1} z_{ip}z_{i1}\tanh(\frac{z_{ip}l_{ip}\underline{w}_{i1}^{-1}z_{i1}}{\tau_{ip}^{(1)}}) + 0.2785\tau_{ip}^{(1)}, \tag{6.19}$$

$$l_{ip}(w_{i1}^{-1}+1)z_{ip}C\xi_i \le l_{ip}\underline{w}_{i1}^{-1} z_{ip}C\xi_{i1}\tanh(\frac{z_{ip}l_{ip}\underline{w}_{i1}^{-1}C\xi_{i1}}{\tau_{ip}^{(2)}}) + 0.2785\tau_{ip}^{(2)}, \tag{6.20}$$

and

$$z_{ip}z_{i,p+1} \le \frac{1}{4\tau^{(3)}} z_{ip}^2 + \tau_{ip}^{(3)} z_{i,p+1}^2, \tag{6.21}$$

where $\tau_{ip}^{(l)}$ for $l = 1, 2, 3$ are positive constants.

Let

$$\begin{aligned}G_{ip}(X_{ip}) =&l_{ip}\underline{w}_{i1}^{-1} z_{i1}\tanh(\frac{z_{ip}l_{ip}\underline{w}_{i1}^{-1}z_{i1}}{\tau_{ip}^{(1)}}) + l_{ip}\underline{w}_{i1}^{-1}C\xi_{i1}\tanh(\frac{z_{ip}l_{ip}\underline{w}_{i1}^{-1}C\xi_{i1}}{\tau_{ip}^{(1)}})\\ &+ \left(\tau_{i,p-1}^{(3)} + \frac{1}{4\tau^{(3)}}\right)z_{ip} - \sum_{j=1}^{p-1}\frac{\partial\alpha_{i,p-1}}{\partial\hat{x}_{ij}}\left[\hat{x}_{i,j+1} + l_{ij}\left(\breve{x}_{i1} - \hat{x}_{i1}\right)\right]\\ &- \sum_{j=0}^{p-1}\frac{\partial\alpha_{i,p-1}}{\partial\xi_{i1}^{(j)}}\xi_{i1}^{(j+1)} - \sum_{j=1}^{p-1}\frac{\partial\alpha_{i,p-1}}{\partial\hat{\vartheta}_{ij}}\dot{\hat{\vartheta}}_{ij},\end{aligned} \tag{6.22}$$

where $X_{ip} = [\breve{x}_{i1}, \hat{\bar{x}}_{ip}, \xi_{i1}, \dot{\xi}_{i1}, \ldots, \xi_{i1}^{(p)}, \hat{\vartheta}_{i1}, \ldots, \hat{\vartheta}_{i,p-1}]^T$.

Thus,

$$\begin{aligned}V_{ip} \le &- c_{i0}^{(1)} e_i^T e_i - \sum_{j=1}^{p-1}\gamma_{ij}^{(1)} z_{ij}^2 + \sum_{j=1}^{p-1}\gamma_{ij}^{(2)}\tilde{\vartheta}_{ij}\hat{\vartheta}_{ij} + z_{ip}\alpha_{ip} + z_{ip}G_{ip}(X_{ip})\\ &- \tilde{\vartheta}_{ip}\dot{\hat{\vartheta}}_{ip} + \tau_{ip}^{(3)} z_{i,p+1}^2 + M_{i,p-1} + 0.2785\tau_{ip}^{(1)} + 0.2785\tau_{ip}^{(2)}.\end{aligned} \tag{6.23}$$

Utilizing an FLS $\theta_{ip}^T\phi_{ip}$ to approximate the unknown function G_{ip}, one gets $G_{ip} = \theta_{ip}^T\phi_{ip} + \epsilon_{ip}$, where ϵ_{ip} is the estimation error satisfying $|\epsilon_{ip}| \le \bar{\epsilon}_{ip}$ with $\bar{\epsilon}_{ip}$ being a constant. Thus,

$$z_{ip}G_{ip} = z_{ip}(\theta_{ip}^T\phi_{ip} + \epsilon_{ip})$$

$$\leq \vartheta_{ip}\varphi_{ip}z_{ip}\tanh(\frac{z_{ip}\varphi_{ip}}{\gamma_{ip}^{(3)}}) + 0.2875\gamma_{ip}^{(3)}\vartheta_{ip}, \tag{6.24}$$

where $\vartheta_{ip} = \max\{\bar{\epsilon}_{ip}, \|\theta_{ip}\|\}$, $\varphi_{ip} = 1 + \|\phi_{ip}\|$, and $\gamma_{ip}^{(3)} > 0$ is a design parameter.

The virtual controller α_{ip} and the adaptive law $\dot{\hat{\vartheta}}_{ip}$ are designed as

$$\alpha_{ip} = -\gamma_{ip}^{(1)}z_{ip} - \hat{\vartheta}_{ip}\varphi_{ip}\tanh(\frac{z_{ip}\varphi_{ip}}{\gamma_{ip}^{(3)}}) \tag{6.25}$$

and

$$\dot{\hat{\vartheta}}_{ip} = -\gamma_{ip}^{(2)}\hat{\vartheta}_{ip} + z_{ip}\varphi_{ip}\tanh(\frac{z_{ip}\varphi_{ip}}{\gamma_{ip}^{(3)}}), \tag{6.26}$$

where $\gamma_{ip}^{(1)}, \gamma_{ip}^{(2)}$ are positive design parameters.

In accordance with (6.24)–(6.26), it can be obtained that

$$\dot{V}_{ip} \leq -c_{i0}^{(1)}e_i^T e_i - \sum_{j=1}^{p}\gamma_{ij}^{(1)}z_{ij}^2 + \sum_{j=1}^{p}\gamma_{ij}\tilde{\vartheta}_{ij}\hat{\vartheta}_{ij} + \tau_{ip}^{(3)}z_{i,p+1}^2 + M_{ip}, \tag{6.27}$$

where $M_{ip} = M_{i,p-1} + 0.2785\tau_{ip}^{(1)} + 0.2785\tau_{ip}^{(2)} + 0.2785\gamma_{ip}^{(3)}\vartheta_{ip}$.

Step n: From (5.1) and (6.1), one gets that

$$\begin{aligned}\dot{z}_{in} =& \dot{\hat{x}}_{in} - \dot{\alpha}_{i,n-1}\\ =& u_{iD} + l_{in}(\breve{x}_{i1} - \hat{x}_{i1}) - \dot{\alpha}_{i,n-1}.\end{aligned} \tag{6.28}$$

Construct the following Lyapunov function candidate V_{in} as

$$V_{in} = V_{i,n-1} + \frac{1}{2}z_{in}^2 + \frac{1}{2}\tilde{\vartheta}_{in}^2, \tag{6.29}$$

where $\tilde{\vartheta}_{in} = \vartheta_{in} - \hat{\vartheta}_{in}$ and $\hat{\vartheta}_{in}$ is the estimation of ϑ_{in}. The definition of ϑ_{in} will be given later.

Its time derivative can be calculated as

$$\begin{aligned}\dot{V}_{in} =& -c_{i0}^{(1)}e_i^T e_i - \sum_{j=1}^{n-1}\gamma_{ij}^{(1)}z_{ij}^2 + \sum_{j=1}^{n-1}\gamma_{ij}\tilde{\vartheta}_{ij}\hat{\vartheta}_{ij} + \tau_{i,n-1}^{(3)}z_{in} + M_{i,n-1}\\ &+ z_{in}\Big[\underline{q_i}(1+\rho_i)u_i + p_i + l_{in}(w_{i1}^{-1}+1)(z_{i1} + C\xi_{i1}) - \dot{\alpha}_{i,n-1}\Big)]\\ &- \tilde{\vartheta}_{in}\dot{\hat{\vartheta}}_{in}.\end{aligned} \tag{6.30}$$

From Lemma 2.3, one has

$$l_{in}(w_{i1}^{-1}+1)z_{in}z_{i1} \leq l_{in}\underline{w}_{i1}^{-1}z_{in}z_{i1}\tanh(\frac{z_{in}l_{in}\underline{w}_{i1}^{-1}z_{i1}}{\tau_{in}^{(1)}}) + 0.2785\tau_{in}^{(1)}, \tag{6.31}$$

$$l_{in}(w_{i1}^{-1}+1)z_{in}C\xi_i \leq l_{in}\underline{w}_{i1}^{-1}z_{in}C\xi_{i1}\tanh(\frac{z_{in}l_{in}\underline{w}_{i1}^{-1}C\xi_{i1}}{\tau_{in}^{(2)}}) + 0.2785\tau_{in}^{(2)}, \tag{6.32}$$

$$z_{in}\left[\underline{q}_i\left(\rho_i+1\right)u_i-u_i\right]\leq z_{in}(\bar{q}_i+1)\bar{u}_i\tanh\left(\frac{z_{in}(\bar{q}_i+1)\bar{u}_i}{\tau_{in}^{(3)}}\right)+0.2785\tau_{in}^{(3)},\tag{6.33}$$

and

$$z_{in}p_i\leq z_{in}\bar{p}_i\tanh(\frac{z_{in}\bar{p}_i}{\tau_{in}^{(4)}})+0.2785\tau_{in}^{(4)},\tag{6.34}$$

where $\tau_{in}^{(l)}$ for $l=1,2,3,4$ are positive constants.

Let

$$\begin{aligned}G_{in}(X_{in})=&l_{in}\underline{w}_{i1}^{-1}z_{i1}\tanh(\frac{z_{in}l_{in}\underline{w}_{i1}^{-1}z_{i1}}{\tau_{in}^{(1)}})+l_{in}\underline{w}_{i1}^{-1}C\xi_{i1}\tanh(\frac{z_{in}l_{in}\underline{w}_{i1}^{-1}C\xi_{i1}}{\tau_{in}^{(2)}})\\&+\Big(\tau_{i,n-1}^{(3)}+\bar{p}_i\tanh(\frac{z_{in}\bar{p}_i}{\tau_{in}^{(4)}})\Big)z_{in}-\sum_{j=0}^{n-1}\frac{\partial\alpha_{i,n-1}}{\partial\xi_{i1}^{(j)}}\xi_{i1}^{(j+1)}\\&-\sum_{j=1}^{n-1}\frac{\partial\alpha_{i,n-1}}{\partial\hat{\vartheta}_{ij}}\dot{\hat{\vartheta}}_{ij}-\sum_{j=1}^{n-1}\frac{\partial\alpha_{i,n-1}}{\partial\hat{x}_{ij}}\left[\hat{x}_{i,j+1}+l_{ij}\left(\breve{x}_{i1}-\hat{x}_{i1}\right)\right]\\&+(\bar{q}_i+1)\bar{u}_i\tanh\left(\frac{z_{in}(\bar{q}_i+1)\bar{u}_i}{\tau_{in}^{(3)}}\right)+\bar{p}_i\tanh(\frac{z_{in}\bar{p}_i}{\tau_{in}^{(4)}}),\end{aligned}\tag{6.35}$$

where $X_{in}=[\breve{x}_{i1},\hat{\bar{x}}_{in},\xi_{i1},\dot{\xi}_{i1},\ldots,\dot{\xi}_{i1}^{(n)},\hat{\vartheta}_{i1},\ldots,\hat{\vartheta}_{i,n-1}]^T$.

Thus,

$$\begin{aligned}V_{in}\leq&-c_{i0}^{(1)}e_i^Te_i-\sum_{j=1}^{n-1}\gamma_{ij}^{(1)}z_{ij}^2+\sum_{j=1}^{n-1}\gamma_{ij}\tilde{\vartheta}_{ij}\hat{\vartheta}_{ij}+z_{in}u_i+z_{in}G_{in}(X_{in})\\&-\tilde{\vartheta}_{in}\dot{\hat{\vartheta}}_{in}+M_{i,n-1}+0.2785\tau_{in}^{(1)}+0.2785\tau_{in}^{(2)}+0.2785\tau_{in}^{(3)}\\&+0.2785\tau_{in}^{(4)}.\end{aligned}\tag{6.36}$$

Applying an FLS $\theta_{in}^T\phi_{in}$ to approximate the unknown function G_{in}, one gets $G_{in}=\theta_{in}^T\phi_{in}+\epsilon_{in}$, where ϵ_{in} is the estimation error satisfying $|\epsilon_{in}|\leq\bar{\epsilon}_{in}$ with $\bar{\epsilon}_{in}$ being a positive constant.

Thus,

$$\begin{aligned}z_{in}G_{in}=&z_{in}(\theta_{in}^T\phi_{in}+\epsilon_{in})\\\leq&\vartheta_{in}\varphi_{in}z_{in}\tanh(\frac{z_{in}\varphi_{in}}{\gamma_{in}^{(3)}})+0.2875\gamma_{in}^{(3)}\vartheta_{in},\end{aligned}\tag{6.37}$$

where $\vartheta_{in}=\max\{\bar{\epsilon}_{in},\|\theta_{in}\|\}$, $\varphi_{in}=1+\|\phi_{in}\|$, and $\gamma_{in}^{(3)}>0$ is a design parameter.

The dead-zone input u_i and the adaptive law $\dot{\hat{\vartheta}}_{in}$ are designed as

$$u_i=-\gamma_{in}^{(1)}z_{in}-\hat{\vartheta}_{in}\varphi_{in}\tanh(\frac{z_{in}\varphi_{in}}{\gamma_{in}^{(3)}})\tag{6.38}$$

and

$$\dot{\hat{\vartheta}}_{in} = -\gamma_{in}^{(2)}\hat{\vartheta}_{in} + z_{in}\varphi_{in}\tanh(\frac{z_{in}\varphi_{in}}{\gamma_{in}^{(3)}}), \tag{6.39}$$

where $\gamma_{in}^{(1)}, \gamma_{in}^{(2)}$ are positive design parameters.

In accordance with (6.35)–(6.39), it can be obtained that

$$\dot{V}_{in} \leq -c_{i0}^{(1)} e_i^T e_i - \sum_{j=1}^{n} \gamma_{ij}^{(1)} z_{ij}^2 + \sum_{j=1}^{n} \gamma_{ij}\tilde{\vartheta}_{ij}\hat{\vartheta}_{ij} + M_{in}, \tag{6.40}$$

where $M_{in} = M_{i,n-1} + 0.2785\tau_{in}^{(1)} + 0.2785\tau_{in}^{(2)} + 0.2785\tau_{in}^{(3)} + 0.2785\tau_{in}^{(4)} + 0.2785\gamma_{in}^{(3)}\vartheta_{in}$.

7. Main results

Theorem 7.1. *Consider the MAS* (3.1) *with the deception attacks, the DoS attacks, and the dead zone. Under Assumptions 3.1–3.6, provided that the conditions in Theorems 4.1 and 4.2 are satisfied, by employing adaptive laws* (6.14), (6.26), (6.39) *and virtual controllers* (6.13), (6.25), (6.38), *the following properties are ensured:*

1) All variables in the controlled MAS are bounded;

2) Tracking error $y_i - y_0$ $(i = 1, 2, \ldots, N)$ converges to a neighborhood of the origin.

Proof: Construct the Lyapunov function V as

$$V = \sum_{i=1}^{N} V_{in}. \tag{7.1}$$

From (6.40), one obtains that

$$\dot{V} \leq -\sum_{i=1}^{N} c_{i0}^{(1)} e_i^T e_i - \sum_{j=1}^{n} \gamma_{ij}^{(1)} z_{ij}^2 + \sum_{j=1}^{n} \gamma_{ij}^{(2)}\tilde{\vartheta}_{ij}\hat{\vartheta}_{ij} + M_{in}. \tag{7.2}$$

Using Young's inequality, one has

$$\tilde{\vartheta}_{ij}\hat{\vartheta}_{ij} \leq -\frac{\tilde{\vartheta}_{ij}^2}{2} + \frac{\vartheta_{ij}^2}{2}. \tag{7.3}$$

Substituting (7.3) into (7.2), we have

$$\begin{aligned}\dot{V} &\leq -\sum_{i=1}^{n} c_{i0}^{(1)} e_i^T e_i - \sum_{j=1}^{n} \gamma_{ij}^{(1)} z_{ij}^2 - \sum_{j=1}^{n} \frac{\gamma_{ij}^{(2)}}{2}\tilde{\vartheta}_{ij}^2 + \sum_{j=1}^{n} \frac{\gamma_{ij}^{(2)}}{2}\vartheta_{ij}^2 + M_{in} \\ &\leq -cV + M,\end{aligned} \tag{7.4}$$

where $c = \min\{c_{i0}^{(1)}, \gamma_{ij}^{(1)}, \frac{\gamma_{ij}^{(2)}}{2}\}$ and $M = M_{in} + \sum_{j=1}^{n} \frac{\gamma_{ij}^{(2)}}{2}\vartheta_{ij}^2$.

Integrating both sides of (7.4) from 0 to t results in

$$0 \leq V \leq V(0)e^{-ct} + \frac{M}{c}. \tag{7.5}$$

Hence, we obtain that $\|e_i\| \leq \sqrt{\frac{a_i M}{c\lambda_{\min}(P_i)}}$, $\|z_i\| \leq \sqrt{\frac{2M}{c}}$ with $z_i = [z_{i1}, ..., z_{in}]^T$, $\|\tilde{\vartheta}_{i1}\| \leq \sqrt{\frac{2\bar{w}_{i1}M}{c}}$, and $\|\tilde{\vartheta}_{iq}\| \leq \sqrt{\frac{2M}{c}}, q = 2, \ldots, n$, as $t \to +\infty$. Therefore, all variables in the controlled MAS are bounded. Since

$$\begin{aligned}
|y_i - y_0| =& |x_{i1} - C\eta_0| = |\frac{z_{i1} + C\xi_{i1} - C\eta_0 + C\eta_0}{w_{i1}} - C\eta_0| \\
=& |\frac{z_{i1} + C(\xi_{i1} - \eta_0)}{w_{i1}} + \left(\frac{1}{w_{i1}} - 1\right)C\eta_0| \\
\leq& \frac{1}{\underline{w}_{i1}}|z_{i1}| + \|C\|\|\xi_{i1} - \eta_0\| + (\frac{1}{\underline{w}_{i1}} + 1)\|C\|\|\eta_0\|,
\end{aligned}$$

along with the boundedness of z_{i1} and η_0 and the exponential convergence of ξ_{i1}, it follows that $|y_i - y_0|$ converges to a neighborhood containing the origin. This completes the proof.

Remark 4. *The computational complexity of the algorithm can be analyzed from the following aspects: First, high-dimensional LMIs can be solved via offline computation without occupying online computing resources. Second, for large-scale MASs, the proposed algorithm features a distributed property, where each agent only involves the local information of neighboring agents through distributed computation, thus greatly reducing the computational burden. Third, for high-dimensional estimated parameter vectors such as those in FLSs, the 2-norm is introduced to convert the high-dimensional estimated parameter vectors into scalars, which significantly lowers the computational complexity of the algorithm.*

Remark 5. *Even under milder conditions, e.g., in the absence of external disturbances, it is difficult to achieve asymptotic tracking performance. This is due to the difficulty in accurately estimating the uncertain nonlinear dynamics existing in the system. However, we can adjust the design parameters to minimize the neighborhood around the origin as much as possible.*

8. Simulation

In this section, the effectiveness of the proposed method is illustrated through computer simulation.

Consider an MAS including a leader and four one-link manipulators. The interconnected relationship among these five agents is depicted in Figure 1. The four manipulators are described by

$$\tau_i^{(1)}\ddot{p}_i + \tau_i^{(2)}\dot{p}_i + \tau_i^{(3)}\sin(p_i) = u_i + \varpi_i, \quad i = 1, 2, 3, 4, \tag{8.1}$$

where $\tau_i^{(1)}, \tau_i^{(2)}$, and $\tau_i^{(3)}$ are unknown constants. $\ddot{p}_i$, $\dot{p}_i$, and p_i are the link acceleration, the angular velocity and the angle of the rigid link, respectively. ϖ_i is the torque disturbance.

Letting $x_{i1} = p_i$ and $x_{i2} = \dot{p}_1$, from (8.1), one has

$$\begin{cases}
\dot{x}_{i1} = x_{i2}, \\
\dot{x}_{i2} = \frac{1}{\tau_i^{(1)}}u_i(t) - \frac{\tau_i^{(2)}}{\tau_i^{(1)}}x_{i2} - \frac{\tau_i^{(3)}}{\tau_i^{(1)}}\sin(x_{i1}) + \frac{1}{\tau_i^{(1)}}\varpi_i, \\
y_i = x_{i1}, \quad i = 1, 2, 3, 4.
\end{cases} \tag{8.2}$$

Here, as an example, let $\tau_i^{(1)} = 1, \tau_i^{(2)} = 1, \tau_i^{(3)} = 0.01$, and $\varpi_i = 0.1\cos(t)$.

The fuzzy membership functions are selected as $\mu_{F_p^l}(x_p) = \exp(-(x_p + 2.5 - 0.5l)^2/8)$ for $l = 1, 2, ..., 9$. Thus, the fuzzy basis functions can be obtained as

$$\varphi_{i1}^{(l)}(X_{i1}) = \frac{\prod_{p=1}^{4} \mu_{F_p^l}(X_{11}^p)}{\sum_{l=1}^{9} \left(\prod_{p=1}^{4} \mu_{F_p^l}(X_{11}^p)\right)}, \quad i = 1, 2, 3, 4, l = 1, 2, \ldots, 9 \tag{8.3}$$

and

$$\varphi_{i2}^{(l)}(X_{i2}) = \frac{\prod_{p=1}^{7} \mu_{F_p^l}(X_{i2}^p)}{\sum_{l=1}^{9} \left(\prod_{p=1}^{7} \mu_{F_p^l}(X_{i2}^p)\right)}, \quad i = 1, 2, 3, 4, l = 1, 2, \ldots, 9, \tag{8.4}$$

where

$$\begin{aligned}
X_{11} &= [X_{11}^1, X_{11}^2, X_{11}^3, X_{11}^4]^T = [\breve{x}_{11}, \hat{x}_{11}, \xi_{11}, \dot{\xi}_{11}]^T,\\
X_{21} &= [X_{21}^1, X_{21}^2, X_{21}^3, X_{21}^4]^T = [\breve{x}_{21}, \hat{x}_{21}, \xi_{21}, \dot{\xi}_{21}]^T,\\
X_{31} &= [X_{31}^1, X_{31}^2, X_{31}^3, X_{31}^4]^T = [\breve{x}_{31}, \hat{x}_{31}, \xi_{31}, \dot{\xi}_{31}]^T,\\
X_{41} &= [X_{41}^1, X_{41}^2, X_{41}^3, X_{41}^4]^T = [\breve{x}_{41}, \hat{x}_{41}, \xi_{41}, \dot{\xi}_{41}]^T,\\
X_{12} &= [X_{12}^1, X_{12}^2, \ldots, X_{12}^7]^T = [\breve{x}_{11}, \hat{x}_{11}, \hat{x}_{12}, \xi_{11}, \dot{\xi}_{11}, \xi_{11}^{(2)}, \hat{\vartheta}_{11}]^T,\\
X_{22} &= [X_{22}^1, X_{22}^2, \ldots, X_{22}^7]^T = [\breve{x}_{21}, \hat{x}_{21}, \hat{x}_{22}, \xi_{21}, \dot{\xi}_{21}, \xi_{21}^{(2)}, \hat{\vartheta}_{21}]^T,\\
X_{32} &= [X_{32}^1, X_{32}^2, \ldots, X_{32}^7]^T = [\breve{x}_{31}, \hat{x}_{31}, \hat{x}_{32}, \xi_{31}, \dot{\xi}_{31}, \xi_{31}^{(2)}, \hat{\vartheta}_{31}]^T,\\
X_{42} &= [X_{42}^1, X_{42}^2, \ldots, X_{42}^7]^T = [\breve{x}_{41}, \hat{x}_{41}, \hat{x}_{42}, \xi_{41}, \dot{\xi}_{41}, \xi_{41}^{(2)}, \hat{\vartheta}_{41}]^T,
\end{aligned}$$

and the fuzzy basis function vectors are given by $\varphi_{ij} = [\varphi_{ij}^{(1)}(X_{ij}), \ldots, \varphi_{ij}^{(9)}(X_{ij})]^T$ for $i = 1, \ldots, 4$ and $j = 1, 2$.

The leader agent is described by the following dynamical equation:

$$\begin{cases} \dot{\eta}_0 &= A\eta_0, \\ y_0 &= C\eta_0, \end{cases}$$

with $A = \begin{bmatrix} 0 & 0.1 \\ -0.1 & 0 \end{bmatrix}$ and $C = \begin{bmatrix} 1 & 0 \end{bmatrix}$.

The time-delay τ_p is randomly generated within the time interval $[0.001, 0.1]$, thus $\underline{\tau} = 0.001$ and $\bar{\tau} = 0.2$ by setting the sampling period $h = 0.1$. Solving the LMIs (B.1) and (B.2) in Theorem 7.1 with $a = 0.5$, $b = 5$, and $\mu = 10$, we obtain the gain matrix K in (4.3). The DoS attack intervals are selected as $\{[0.01, 0.21) \cup [0.9, 1.2) \cup [2.2, 2.4) \cup [3.1, 3.4) \cup [3.7, 3.8) \cup [4.9, 5.1) \cup [6.9, 7.1) \cup [7.5, 7.8) \cup [8.9, 9.1) \cup [10.5, 10.7) \cup [11.1, 11.3)\}$. The main parameters are selected as $l_{i1} = l_{i2} = 5$, $\gamma_{i1}^{(1)} = \gamma_{i2}^{(1)} = 50$, $\gamma_{i1}^{(2)} = \gamma_{i2}^{(2)} = 50$, $\gamma_{i1}^{(3)} = \gamma_{i2}^{(3)} = 5$, $b_{il} = 0.1, b_{ir} = 0.1$, $q_{ir} = 0.2$, and $q_{il} = 0.2$ for $i = 1, 2, 3, 4$, and $\sigma = 2.5$.

Figure 1. Interconnected graph.

The simulation is conducted within 10 seconds, and the simulation results are presented in Figures 2–7 to validate the effectiveness of the proposed control scheme in the presence of deception attacks and DoS attacks. The tracking performances of the system outputs and the observer outputs with respect to the leader signal are shown in Figures 2 and 3, respectively. It can be observed that the output signals track the leader signal well. Figure 4 depicts the curves of the state estimation errors $\bar{\eta}_i$, $i = 1, \ldots, 4$. As shown in Figure 4, the estimation errors quickly converge to a small neighborhood of the origin, demonstrating the effectiveness of the proposed distributed estimator. Figure 5 shows the evolution of the adaptive parameters $\hat{\vartheta}_{ij}$. These parameters are updated online via the designed adaptive laws and eventually converge to bounded values, demonstrating the effectiveness of the adaptive mechanism in compensating for system uncertainties and attack-induced disturbances. Figure 6 presents the curves of dead-zone controller u_{iD} and the control input u_i. The control signal remains zero within the dead-zone range and varies continuously outside of it, conforming to the physical characteristics of the actuator, with no significant chattering observed. Figure 7 displays the curves of observer errors for four agents. The observer errors converge rapidly in the initial phase and exhibit minor fluctuations during attack periods, which further demonstrates the effectiveness of the observer design.

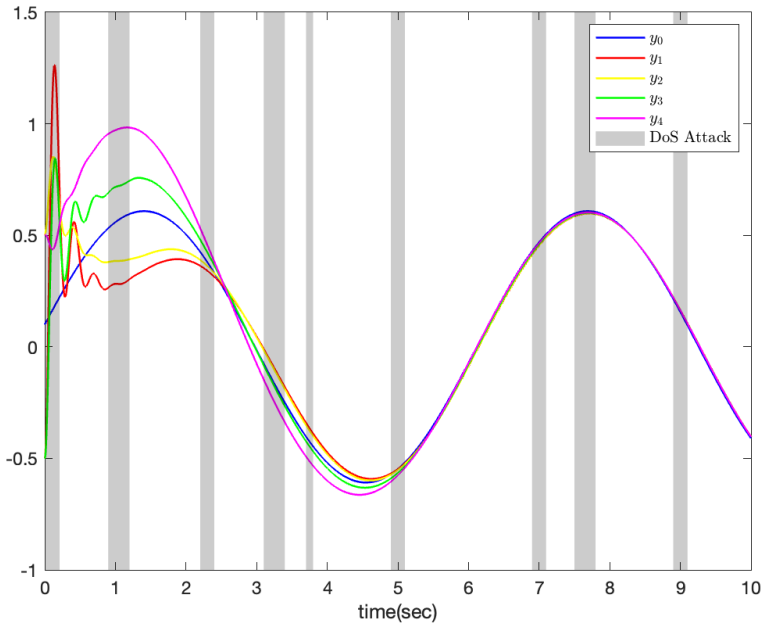

Figure 2. The trajectories of y_0 and y_i with DoS attacks.

Remark 6. *Unlike [25, 27] that only target a single type of attack and neglect deception attacks and input dead zones, the method proposed in this paper can simultaneously suppress the adverse effects caused by deception attacks, DoS attacks, and asymmetric input dead zones; different from [13,14] that rely on prior knowledge such as dead-zone boundary parameters to achieve compensation, the fuzzy adaptive scheme proposed in this paper can accomplish effective dead-zone compensation without any parameter calibration. In contrast to the designs of [24, 30], which adopt simple leader models, this paper introduces a more general high-order leader dynamic model that is more consistent with*

practical application scenarios; unlike the methods [34] using continuous state feedback, this paper processes sampled data by introducing artificial time delay and then constructs a distributed leader-state estimator, which is more in line with the requirements of practical engineering applications.

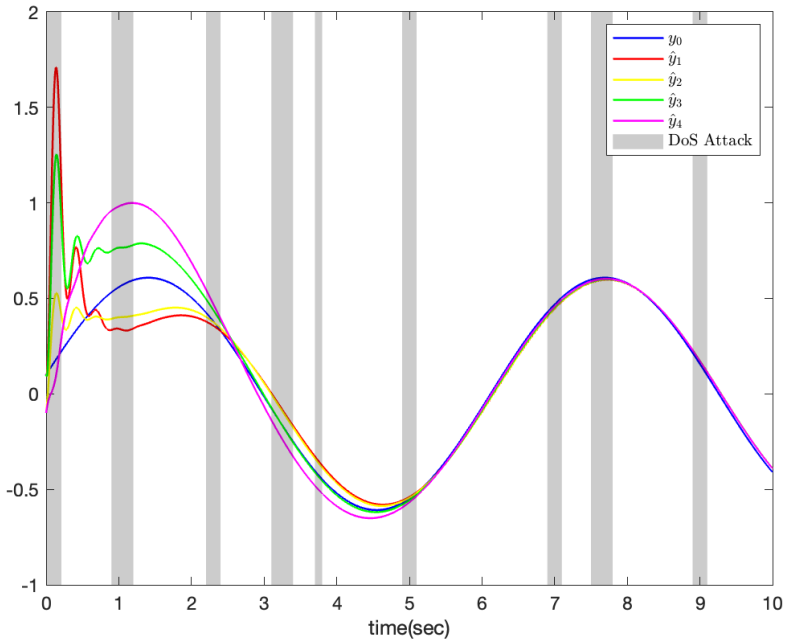

Figure 3. The trajectories of y_0 and $\hat{y}_i$ with DoS attacks.

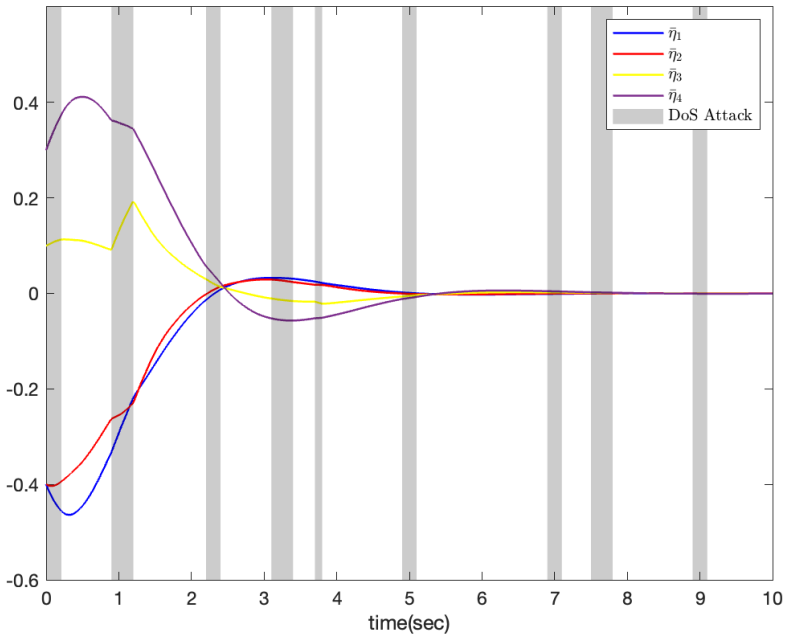

Figure 4. The curves of estimation error $\bar{\eta}_i$ with DoS attacks.

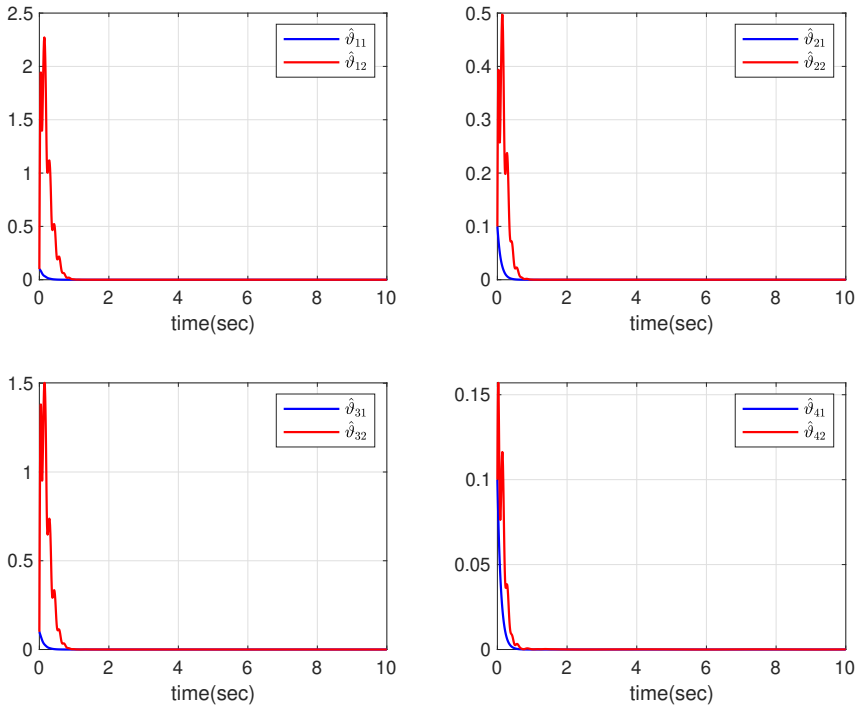

Figure 5. The curves of adaptive parameter $\hat{\vartheta}_{ij}$.

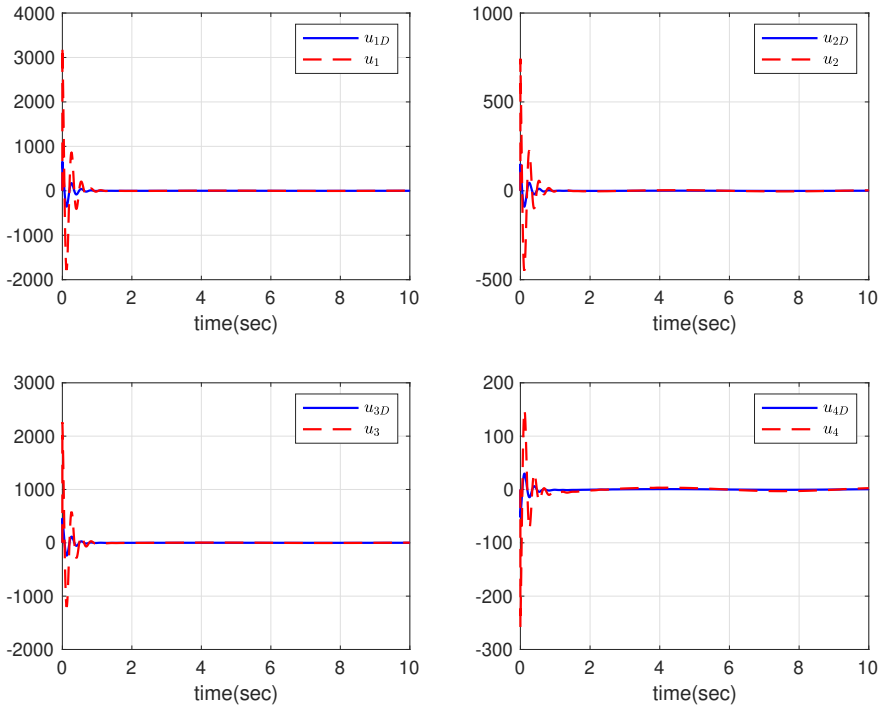

Figure 6. The curves of controller u_{iD} and control input u_i.

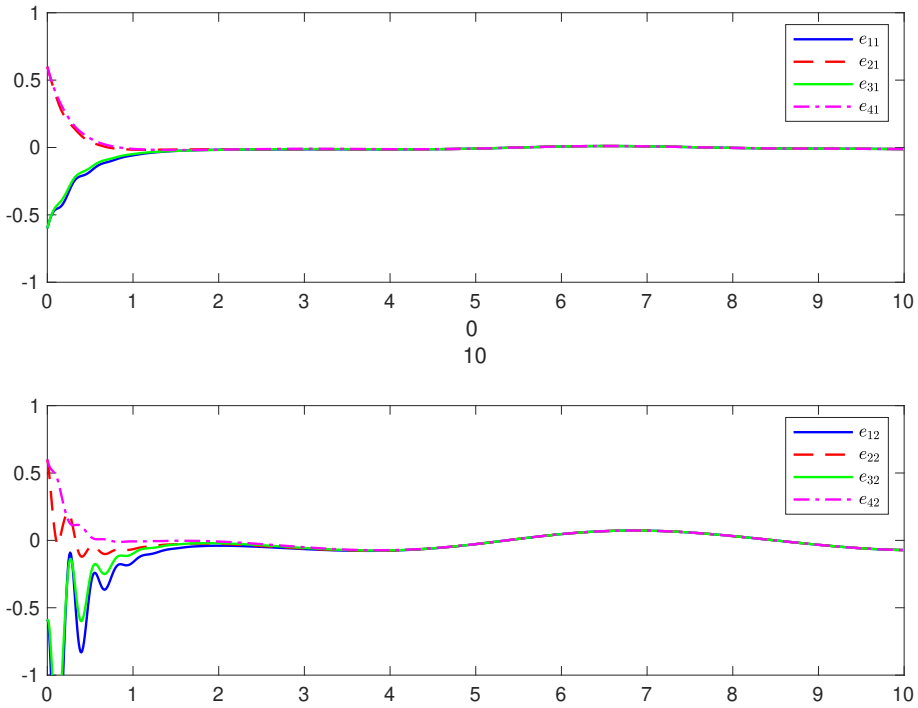

Figure 7. The curves of observer errors.

9. Conclusions

This study proposes an adaptive tracking scheme for nonlinear MASs subject to deception attacks, DoS attacks, and input dead zones. The scheme integrates a distributed state estimator, a fuzzy state observer, and adaptive backstepping control and employs FLSs to approximate unknown nonlinear dynamics. This method enables the estimation of the leader's state, compensates for the effects induced by attacks and disturbances, and ensures the boundedness of all signals in the closed-loop system as well as the convergence of tracking errors to a small neighborhood of the origin. Simulation results verify the effectiveness of the proposed method. Future work will extend this research to constrained scenarios and investigate the fixed-time stability and predefined-time stability of the closed-loop system.

Use of AI tools declaration

The authors declare they have not used Artificial Intelligence (AI) tools in the creation of this article.

Conflict of interest

The authors declare there is no conflicts of interest.

References

1. P. Leitão, S. Karnouskos, L. Ribeiro, J. Lee, T. Strasser, A. W. Colombo, Smart agents in industrial cyber-physical systems, *Proceedings of the IEEE*, **104** (2016), 1086–1101. https://doi.org/10.1109/JPROC.2016.2521931
2. D. Zhang, G. Feng, Y. Shi, D. Srinivasan, Physical safety and cyber security analysis of multi-agent systems: A survey of recent advances, *IEEE/CAA J. Autom. Sin.*, **8** (2021), 319–333. https://doi.org/10.1109/JAS.2021.1003820
3. K. Zhang, Y. Shi, S. Karnouskos, T. Sauter, H. Fang, A. W. Colombo, Advancements in industrial cyber-physical systems: An overview and perspectives, *IEEE Trans. Ind. Inf.*, **19** (2023), 716–729. https://doi.org/10.1109/TII.2022.3199481
4. G. E. M. Abro, Z. A. Ali, R. J. Masood, Synergistic UAV motion: A comprehensive review on advancing multi-agent coordination, *ICCK Trans. Sens. Commun. Control*, **1** (2024), 72–88. https://doi.org/10.62762/TSCC.2024.211408
5. Z. Qian, W. Lyu, Y. Dai, J. Xu, A consensus-based model predictive control with optimized line-of-sight guidance for formation trajectory tracking of autonomous underwater vehicles, *J. Intell. Robotic Syst.*, **106** (2022), 15. https://doi.org/10.1007/s10846-022-01710-4
6. H. Çeker, J. Zhuang, S. Upadhyaya, Q. D. La, B. Soong, Deception-based game theoretical approach to mitigate DoS attacks, in *Decision and Game Theory for Security* , (2016), 18–38. https://doi.org/10.1007/978-3-319-47413-7_2
7. A. Kazemy, J. Lam, X. Zhang, Event-triggered output feedback synchronization of master–slave neural networks under deception attacks, *IEEE Trans. Neural Networks Learn. Syst.*, **33** (2022), 952–961. https://doi.org/10.1109/TNNLS.2020.3030638
8. N. Zhao, Y. Tian, H. Zhang, E. Herrera-Viedma, Learning-based adaptive fuzzy output feedback control for MIMO nonlinear systems with deception attacks and input saturation, *IEEE Trans. Fuzzy Syst.*, **32** (2024), 2850–2862. https://doi.org/10.1109/TFUZZ.2024.3363839
9. C. Deng, D. Yue, W. Che, X. Xie, Cooperative fault-tolerant control for a class of nonlinear MASs by resilient learning approach, *IEEE Trans. Neural Networks Learn. Syst.*, **35** (2024), 670–679. https://doi.org/10.1109/TNNLS.2022.3176392
10. M. Zhao, J. Xi, L. Wang, C. Wang, Y. Zheng, Fully distributed secure tracking for leader-following nonlinear multiagent systems with multi-link sequence scaling attacks, *IEEE Control Syst. Lett.*, **8** (2024), 327–332. https://doi.org/10.1109/LCSYS.2024.3375156
11. F. Cheng, H. Liang, H. Wang, G. Zong, N. Xu, Adaptive neural self-triggered bipartite fault-tolerant control for nonlinear MASs with dead-zone constraints, *IEEE Trans. Autom. Sci. Eng.*, **20** (2023), 1663–1674. https://doi.org/10.1109/TASE.2022.3184022
12. Y. Li, G. Yang, Adaptive fuzzy decentralized control for a class of large-scale nonlinear systems with actuator faults and unknown dead zones, *IEEE Trans. Syst. Man Cybern. Syst.*, **47** (2017), 729–740. https://doi.org/10.1109/TSMC.2016.2521824
13. X. Jia, S. Xu, Z. Zhang, G. Cui, Output feedback robust stabilisation for uncertain non-linear systems with dead-zone input, *IET Control Theory Appl.*, **14** (2020), 1828–1836. https://doi.org/10.1049/iet-cta.2020.0107

14. Z. Ma, S. Tong, Nonlinear filters-based adaptive fuzzy control of strict-feedback nonlinear systems with unknown asymmetric dead-zone output, *IEEE Trans. Autom. Sci. Eng.*, **21** (2024), 5099–5109. https://doi.org/10.1109/TASE.2023.3308528

15. R. Shahnazi, Cooperative neuro adaptive control of leader following uncertain multi-agent systems with unknown hysteresis and dead-zone, *J. Syst. Sci. Complex*, **33** (2020), 312–332. https://doi.org/10.1007/s11424-020-8198-9

16. D. Liu, Z. Liu, C. L. P. Chen, Y. Zhang, Distributed adaptive neural control for uncertain multi-agent systems with unknown actuator failures and unknown dead zones, *Nonlinear Dyn.*, **99** (2020), 1001–1017. https://doi.org/10.1007/s11071-019-05321-x

17. X. Hou, H. Wu, J. Cao, Practical finite-time synchronization for Lur'e systems with performance constraint and actuator faults: A memory-based quantized dynamic event-triggered control strategy, *Appl. Math. Comput.*, **487** (2025), 129108. https://doi.org/10.1016/j.amc.2024.129108

18. H. Zeng, Z. Zhu, T. Peng, W. Wang, X. Zhang, Robust tracking control design for a class of nonlinear networked control systems considering bounded package dropouts and external disturbance, *IEEE Trans. Fuzzy Syst.*, **32** (2024), 3608–3617. https://doi.org/10.1109/TFUZZ.2024.3377799

19. D. Chwa, H. Kwon, Nonlinear robust control of unknown robot manipulator systems with actuators and disturbances using system identification and integral sliding mode disturbance observer, *IEEE Access*, **10** (2022), 35410–35421. https://doi.org/10.1109/ACCESS.2022.3163306

20. X. Zhao, H. Wu, J. Cao, L. Wang, Prescribed-time synchronization for complex dynamic networks of piecewise smooth systems: a hybrid event-triggering control approach, *Qual. Theory Dyn. Syst.*, **24** (2025), 11. https://doi.org/10.1007/s12346-024-01166-x

21. Y. Jiang, C. Yang, H. Ma, A review of fuzzy logic and neural network based intelligent control design for discrete-time systems, *Discrete Dyn. Nat. Soc.*, **2016** (2016), 7217364. https://doi.org/10.1155/2016/7217364

22. K. Gurney, *An Introduction to Neural Networks*, 1st edition, CRC Press, 1997. https://doi.org/10.1201/9781315273570

23. P. Cheng, S. He, G. Xiao, W. Zhang, ESO-based control for 2-D networked control systems with Markov-type DoS attacks, *IEEE Trans. Network Sci. Eng.*, **12** (2025), 4452–4461. https://doi.org/10.1109/TNSE.2025.3572098

24. Y. Liu, C. Deng, X. Xie, W. Che, L. Zhang, S. Fan, Cooperative observer-based fuzzy tracking control for nonlinear MASs under DoS attacks, *IEEE Trans. Fuzzy Syst.*, **32** (2024), 767–777. https://doi.org/10.1109/TFUZZ.2023.3306372

25. H. Zhou, S. Tong, Fuzzy adaptive event-triggered resilient formation control for nonlinear multiagent systems under DoS attacks and input saturation, *IEEE Trans. Syst. Man Cybern. Syst.*, **54** (2024), 3665–3674. https://doi.org/10.1109/TSMC.2024.3369093

26. C. Deng, M. J. Er, G. Yang, N. Wang, Event-triggered consensus of linear multiagent systems with time-varying communication delays, *IEEE Trans. Cybern.*, **50** (2020), 2916–2925. https://doi.org/10.1109/TCYB.2019.2922740

27. H. Zhou, S. Tong, Fuzzy adaptive resilient formation control for nonlinear multiagent systems subject to DoS attacks, *IEEE Trans. Fuzzy Syst.*, **32** (2024), 1446–1454. https://doi.org/10.1109/TFUZZ.2023.3327140

28. Y. Wang, Y. Yang, L. Wu, Adaptive consensus control of multi-agent systems with dead-zone input, in *2024 14th Asian Control Conference (ASCC)*, (2024), 1103–1108.

29. H. Wu, X. Zhao, L. Wang, J. Cao, Observer-based fixed-time topology identification and synchronization for complex networks via quantized pinning control strategy, *Appl. Math. Comput.*, **507** (2025), 129568. https://doi.org/10.1016/j.amc.2025.129568

30. C. Deng, C. Wen, MAS-based distributed resilient control for a class of cyber-physical systems with communication delays under DoS attacks, *IEEE Trans. Cybern.*, **51** (2021), 2347–2358. https://doi.org/10.1109/TCYB.2020.2972686

31. R. Olfati-Saber, J. A. Fax, R. M. Murray, Consensus and cooperation in networked multi-agent systems, in *Proceedings of the IEEE*, **95** (2007), 215–233. https://doi.org/10.1109/JPROC.2006.887293

32. Y. Shang, B. Chen, C. Lin, Consensus tracking control for distributed nonlinear multiagent systems via adaptive neural backstepping approach, *IEEE Trans. Syst. Man Cybern. Syst.*, **50** (2020), 2436–2444. https://doi.org/10.1109/TSMC.2018.2816928

33. H. Deng, M. Krstic, Output-feedback stochastic nonlinear stabilization, *IEEE Trans. Autom. Control*, **44** (1999), 328–333. https://doi.org/10.1109/9.746260

34. L. Ding, Q. Han, G. Guo, Network-based leader-following consensus for distributed multi-agent systems, *Automatica*, **49** (2013), 2281–2286. https://doi.org/10.1016/j.automatica.2013.04.021

35. P. Park, J. W. Ko, C. Jeong, Reciprocally convex approach to stability of systems with time-varying delays, *Automatica*, **47** (2011), 235–238. https://doi.org/10.1016/j.automatica.2010.10.014

36. N. Wang, Y. Wang, J. H. Park, M. Lv, F. Zhang, Fuzzy adaptive finite-time consensus tracking control of high-order nonlinear multi-agent networks with dead zone, *Nonlinear Dyn.*, **106** (2021), 3363–3378. https://doi.org/10.1007/s11071-021-06956-5

37. Y. Ma, W. Che, C. Deng, Z. Wu, Observer-based event-triggered containment control for MASs under DoS attacks, *IEEE Trans. Cybern.*, **52** (2022), 13156–13167. https://doi.org/10.1109/TCYB.2021.3104178

Appendix A

$$\Phi = \begin{bmatrix} \Phi_{11} & \Phi_{12} & \Phi_{13} & 0 & \Phi_{15} \\ \star & \Phi_{22} & \Phi_{23} & \Phi_{24} & \Phi_{25} \\ \star & \star & \Phi_{33} & \Phi_{34} & 0 \\ \star & \star & \star & \Phi_{44} & 0 \\ \star & \star & \star & \star & \Phi_{55} \end{bmatrix} \tag{A.1}$$

and

$$\Psi = \begin{bmatrix} \Psi_{11} & 0 & \Psi_{13} & 0 & \Psi_{15} \\ \star & \Psi_{22} & \Psi_{23} & \Psi_{24} & 0 \\ \star & \star & \Psi_{33} & \Psi_{34} & 0 \\ \star & \star & \star & \Psi_{44} & 0 \\ \star & \star & \star & \star & \Psi_{55} \end{bmatrix} \tag{A.2}$$

with $\Phi_{11} = P(I_N \otimes A) + (I_N \otimes A)^T P + aP + Q_1 - e^{-a\underline{\tau}} Z_1, \Phi_{12} = -\gamma PK(\mathcal{H} \otimes I_n), \Phi_{13} = e^{-a\underline{\tau}} Z_1, \Phi_{15} = (I_N \otimes A)^T, \Phi_{22} = e^{-a\bar{\tau}}(S^T + S) - 2e^{-a\bar{\tau}} Z_2, \Phi_{23} = e^{-a\bar{\tau}}(Z_2 - S), \Phi_{24} = e^{-a\bar{\tau}}(Z_2 - S^T), \Phi_{25} = -\gamma_i K(\mathcal{H} \otimes I_n)^T, \Phi_{33} = e^{-a\underline{\tau}}(Q_2 - Q_1 - Z_1) - e^{-a\bar{\tau}} Z_2, \Phi_{34} = e^{-a\bar{\tau}} S^T, \Phi_{44} = -e^{-a\bar{\tau}}(Z_2 + Q_2), \Phi_{55} = -(\underline{\tau}^2 Z_1 + \tilde{\tau}^2 Z_2)^{-1}, \Psi_{11} = P(I_N \otimes A) + (I_N \otimes A)^T P - bP + Q_1 - e^{b\underline{\tau}} R_1, \Psi_{13} = e^{b\underline{\tau}} Z_1, \Psi_{15} = (I_N \otimes A)^T, \Psi_{22} = e^{b\bar{\tau}}(S^T + S) - 2e^{b\bar{\tau}} Z_2, \Psi_{23} = e^{b\bar{\tau}}(Z_2 - S), \Psi_{24} = e^{b\bar{\tau}}(Z_2 - S^T), \Psi_{33} = e^{b\underline{\tau}}(Q_2 - Q_1 - Z_1) - e^{b\bar{\tau}} Z_2, \Psi_{34} = e^{b\bar{\tau}} S^T, \Psi_{44} = -e^{b\bar{\tau}}(Z_2 + Q_2)$, and $\Psi_{55} = -(\underline{\tau}^2 Z_1 + \tilde{\tau}^2 Z_2)^{-1}$.

Appendix B

$$\tilde{\Phi} = \begin{bmatrix} \tilde{\Phi}_{11} & \tilde{\Phi}_{12} & \tilde{\Phi}_{13} & 0 & \tilde{\Phi}_{15} \\ \star & \tilde{\Phi}_{22} & \tilde{\Phi}_{23} & \tilde{\Phi}_{24} & \tilde{\Phi}_{25} \\ \star & \star & \tilde{\Phi}_{33} & \tilde{\Phi}_{34} & 0 \\ \star & \star & \star & \tilde{\Phi}_{44} & 0 \\ \star & \star & \star & \star & \tilde{\Phi}_{55} \end{bmatrix} < 0 \tag{B.1}$$

and

$$\tilde{\Psi} = \begin{bmatrix} \tilde{\Psi}_{11} & 0 & \tilde{\Psi}_{13} & 0 & \tilde{\Psi}_{15} \\ \star & \tilde{\Psi}_{22} & \tilde{\Psi}_{23} & \tilde{\Psi}_{24} & 0 \\ \star & \star & \tilde{\Psi}_{33} & \tilde{\Psi}_{34} & 0 \\ \star & \star & \star & \tilde{\Psi}_{44} & 0 \\ \star & \star & \star & \star & \tilde{\Psi}_{55} \end{bmatrix} < 0 \tag{B.2}$$

with $\tilde{\Phi}_{11} = P(I_N \otimes A) + (I_N \otimes A)^T P + aP + Q_1 - e^{-a\underline{\tau}} Z_1, \tilde{\Phi}_{12} = -\gamma(\mathcal{H} \otimes I_n), \tilde{\Phi}_{13} = e^{-a\underline{\tau}} Z_1, \tilde{\Phi}_{15} = (I_N \otimes A)^T P, \tilde{\Phi}_{22} = e^{-a\bar{\tau}}(S^T + S) - 2e^{-a\bar{\tau}} Z_2, \tilde{\Phi}_{23} = e^{-a\bar{\tau}}(Z_2 - S), \tilde{\Phi}_{24} = e^{-a\bar{\tau}}(Z_2 - S^T), \tilde{\Phi}_{25} = -\gamma(\mathcal{H} \otimes I_n)^T P, \tilde{\Phi}_{33} = e^{-a\underline{\tau}}(Q_2 - Q_1 - Z_1) - e^{-a\bar{\tau}} Z_2, \tilde{\Phi}_{34} = e^{-a\bar{\tau}} S^T, \tilde{\Phi}_{44} = -e^{-a\bar{\tau}}(Z_2 + Q_2), \tilde{\Phi}_{55} = \mu^2(\underline{\tau}^2 Z_1 + \tilde{\tau}^2 Z_2) - 2\mu P, \tilde{\Psi}_{11} = P(I_N \otimes A) + (I_N \otimes A)^T P - bP + Q_1 - e^{b\underline{\tau}} R_1, \tilde{\Psi}_{13} = e^{b\underline{\tau}} Z_1, \tilde{\Psi}_{15} = (I_N \otimes A)^T P, \tilde{\Psi}_{22} = e^{b\bar{\tau}}(S^T + S) - 2e^{b\bar{\tau}} Z_2, \tilde{\Psi}_{23} = e^{b\bar{\tau}}(Z_2 - S), \tilde{\Psi}_{24} = e^{b\bar{\tau}}(Z_2 - S^T), \tilde{\Psi}_{33} = e^{b\underline{\tau}}(Q_2 - Q_1 - Z_1) - e^{b\bar{\tau}} Z_2, \tilde{\Psi}_{34} = e^{b\bar{\tau}} S^T, \tilde{\Psi}_{44} = -e^{b\bar{\tau}}(Z_2 + Q_2)$, and $\tilde{\Psi}_{55} = \mu^2(\underline{\tau}^2 Z_1 + \tilde{\tau}^2 Z_2) - 2\mu P$.